**FACULTY OF SCIENCE AND TECHNOLOGY**

# MASTER'S THESIS

| | |
|---|---|
| Study programme / specialisation:<br>Petroleum technology/<br>Production and process | The spring semester, 2023<br><br>Open |
| Author: Gustav Kvitvær | |
| Faculty supervisors: Tina Puntervold<br>Skule Strand<br><br>Laboratory supervisors: Ashraful Islam Khan<br>Aleksandr Mamonov | |
| Thesis title:<br>Low-temperature carbonated water injection for enhanced oil recovery in chalk | |
| Credits (ECTS): 30 | |
| Keywords:<br>Enhanced oil recovery (EOR), carbonated water injection (CWI), $CO_2$, carbon sequestration, Stevns Klint chalk | Pages: 59<br>+ appendix: 6<br><br>Stavanger, 15.06.2023 |

# Acknowledgement

First and foremost, I am grateful for the entire Smart Water group at UiS for granting me the opportunity to work on such an intriguing and innovative topic. I would like to express my gratitude to my supervisors Dr. Tina Puntervold and Dr. Skule Strand. Their expertise and support during the discussion has been invaluable.

I am also grateful to my laboratory supervisors PhD student Ashraful Islam Khan and post-doctoral researcher Aleksandr Mamonov, for all their tremendous help during the lab work. They have not only provided guidance, but also been readily available to address any questions or concerns that arose. I would also like to extend my appreciation to PhD student Mahmood Fani for sharing his experience and enriching my understanding.

Furthermore, I want to acknowledge the collaboration and contributions of my laboratory partners, Thashila Wickrama and Alfred Obo. Thashila Wickrama, thank you for your collaboration on the preparation of the brines and outcrop Stevns Klint chalk core samples. Alfred Obo, I am grateful for our collaborative work on the oil recovery tests through forced imbibition.

This has been an exciting semester with a steep learning curve. I greatly appreciate all the people involved in making this an enjoyable working environment. The friendships I have made during my studies have added value to my experience.

Lastly, I want to thank my parents for their unconditional support throughout my academic pursuit.

# Abstract

The oil industry is still an essential contributor to meeting the continuously increasing global energy demands. As the world looks towards reaching carbon neutrality, new approaches and innovative ideas have never been more important. The best way of minimizing emissions while simultaneously meeting energy demands is to exploit the full potential of mature oil reservoirs close to depletion.

Carbon, capture, use and storage (CCUS) allows for the utilization of these reserves while aligning with the carbon neutrality goals. The use of $CO_2$ as an enhanced oil recovery (EOR) technique is therefore more relevant than ever, as it can be used for carbon sequestration whilst simultaneously improving recovery rate. Pure $CO_2$ injection, as a conventional EOR technique, has undergone extensive testing at both laboratory and reservoir scale. However, it encounters challenges in achieving optimal sweep efficiency. This is primarily due to the low viscosity of $CO_2$ compared to crude oil, resulting in poor mobility ratio.

An emerging EOR technique involves the dissolution of $CO_2$ in water, leading to the formation of a single phase known as carbonated water (CW). The premise of the experimental study is the utilization of CW for EOR. The core material used was the Stevns Klint (SK) chalk outcrop samples, which works as an analogue for North Sea chalk reservoirs, mainly the Ekofisk field.

In total, five cores were used for this study. The oil recovery tests were done through forced imbibition (FI) at both high pressure and low pressure, different injection modes and different temperatures. The effect of acid number (AN) on the wettability was examined. The wettability of two of the cores was measured through spontaneous imbibition (SI) and both exhibited similar slightly water wet characteristics. This suggests that the preparation process was good and that it could work as a wettability representation of the other three cores.

Results from the SI were compared to different oils with lower AN, and the results indicated that the AN directly influences the wettability of the carbonate rock. The oil with lower AN exhibited stronger water wet characteristic. This is in line with previous studies conducted on the matter.

This study found no evidence of temperature effect on total oil recovery during FI when comparing injection at 70℃ and 130℃. The amount of $CO_2$ dissolved in the water did not seem to influence the total recovery, as the trend was similar for the high-pressure set-up compared to the low-pressure set-up. Injecting CW in secondary or tertiary mode did not influence the total recovery, %OOIP, but secondary mode injection required less water injection, therefore less water treatment, thus more economical and environmentally viable.

The main mechanism in this study for carbonated water injection (CWI) seemed to be wettability alteration. The total recovery was similar for experiments with different AN of oil, but the direct recovery from CWI in tertiary mode was higher for the core that had a higher AN and exhibited less natural water wet characteristics before the FI test.

# Table of Contents

**Acknowledgement** ..... I

**Abstract** ..... II

**Table of figures** ..... VI

**List of tables** ..... VIII

**1. Introduction** ..... 1

**1.1 Objectives** ..... 2

**2. Theory and fundamentals** ..... 3

**2.1 Oil recovery mechanism** ..... 3

**2.1.1 Primary stage** ..... 3

**2.1.2 Secondary stage** ..... 3

**2.1.3 Tertiary stage (enhanced oil recovery)** ..... 3

**2.2 Reservoir rock** ..... 5

**2.2.1 Porosity** ..... 5

**2.2.2 Permeability** ..... 5

**2.3 Mineralogy of carbonates** ..... 6

**2.4 Wettability** ..... 7

**2.5 Methods for determining wettability** ..... 8

**2.5.1 Contact angle** ..... 8

**2.5.2 Spontaneous imbibition** ..... 8

**2.5.3 Amott-Harvey** ..... 9

**2.5.4 USBM** ..... 11

**2.6 Displacement forces** ..... 12

**2.6.1 Displacement efficiency** ..... 12

**2.6.2 Fluid mobility through porous media** ..... 13

**2.6.3 Gravity forces** ..... 15

**2.6.4 Viscous forces** ..... 15

**2.6.5 Capillary force** ..... 15

**2.6.6 Capillary number** ..... 16

**2.7 EOR in carbonates** ..... 17

**2.7.1 Smart water injection** ..... 17

**2.7.2 Carbonated water injection** ..... 18

**3. Experimental section** ..... 21

**3.1 Materials** ..... 21

**3.1.1 Core material** ..... 21

**3.1.2 Oil preparation** ..... 22
**3.1.3 Preparation of brines** ..... 23
**3.1.4 Carbonated FW preparation** ..... 24
**3.2 Measurements** ..... 25
**3.2.1 Density** ..... 25
**3.2.2 Viscosity** ..... 26
**3.3 Core preparation** ..... 27
**3.3.1 Core cleaning** ..... 27
**3.3.2 Determining core permeability** ..... 29
**3.3.3 Establishing initial water saturation** ..... 29
**3.3.4 Oil saturation** ..... 31
**3.3.5 Ageing** ..... 31
**3.4 Oil recovery test** ..... 33
**3.4.1 Spontaneous imbibition using FW** ..... 33
**3.4.2 Forced imbibition/viscous flooding using FW, SW, and CFW** ..... 33
**4. Results and discussion** ..... 36
**4.1 Oil recovery at high injection pressure** ..... 37
**4.1.1 Forced imbibition with formation water and carbonated formation water in tertiary mode** ..... 37
**4.2 Oil recovery at low injection pressure** ..... 38
**4.2.1 Forced imbibition with formation water and carbonated formation water in tertiary mode** ..... 39
**4.2.2 Forced imbibition with formation water and carbonated formation water in secondary mode** ..... 39
**4.2.3 Spontaneous imbibition with formation water** ..... 41
**4.2.4 Forced imbibition after spontaneous imbibition with formation water and carbonated formation water in secondary mode** ..... 42
**4.2.5 Forced imbibition after spontaneous imbibition with formation water and carbonated formation water in tertiary mode** ..... 43
**4.3 Comparison of different injection strategies** ..... 44
**4.3.1 Temperature and acid number effect on wettability and oil recovery** ..... 44
**4.3.2 Pressure effect on oil recovery** ..... 47
**4.3.3 Effect of injection mode on oil recovery** ..... 49
**4.3.4 Spontaneous imbibition effect on total oil recovery** ..... 50
**4.3.5 Effect of injection mode after spontaneous imbibition** ..... 52
**5. Conclusion** ..... 54
**6. Research and development** ..... 55

**7. References** ..... 56
**A. Appendix** ..... 59
**A.1 Calculations** ..... 59
**A.1.1 Porosity** ..... 59
**A.1.2 Permeability** ..... 59
**A.2 Oil recovery data** ..... 60
**A.2.1 High injection pressure** ..... 60
**A.2.2 Low injection pressure** ..... 61

# Table of figures

**Figure 2.1** Stages of oil recovery and related recovery factor (Bello et al., 2023) ..... 4
**Figure 2.2** Illustration of water-wet, oil-wet, and mixed-wet system in a porous media ..... 7
**Figure 2.3** Illustration of the different wettability conditions in an oil reservoir (Teklu et al., 2015) .... 8
**Figure 2.4** Example of spontaneous displacement of oil and water for Amott test (Dandekar, 2013) . 10
**Figure 2.5** Centrifuge set-up for USBM test (Dandekar, 2013) ..... 11
**Figure 2.6** Plot of capillary pressure against water saturation used for wettability index (Reed et al., 2014) ..... 12
**Figure 2.7 (a)** Waterflood with M>1 **(b)** Polymer flood at M≤1 (Gbadamosi et al., 2019) ..... 14
**Figure 2.8** Capillary number and relation to residual oil (Craft & Hawkins, 2015b) ..... 17
**Figure 2.9** Illustration of suggested mechanism for wettability alteration **(a)** $Ca2+$ and $SO42-$ active ions. **(b)** $Mg2+$ and $SO42-$ active ions. (Zhang et al., 2007) ..... 18
**Figure 2.10** Solubility of $CO_2$ in pure water as a function of temperature [℃] (Perkins & Innovates, 2003) ..... 19
**Figure 2.11** Oil displacement through **(a)** $CO_2$ injection **(b)** CW injection (Hamouda & Bagalkot, 2019) ..... 19
**Figure 2.12** Phase diagram of $CO_2$ ..... 20
**Figure 3.1** SEM-photo of Stevns Klint chalk (Khan et al., 2023) ..... 21
**Figure 3.2** a) Stevns Klint outcrop chalk b) Drilled cores c) Shaping of desired core diameter after cutting ..... 22
**Figure 3.3** Filtration set-up ..... 24
**Figure 3.4** Anton Paar DMA 4500 density meter used for density measurement ..... 26
**Figure 3.5** Anton Paar MCR 302 rheometer used for viscosity measurements ..... 27
**Figure 3.6** Core cleaning set-up ..... 28
**Figure 3.7** Example of produced water with $BaSO4$ precipitation (left) and without $BaSO4$ precipitation (right) ..... 29
**Figure 3.8** Set-up used for water saturation ..... 30
**Figure 3.9** Desiccator used for slow drying the cores until target weight was reached ..... 31
**Figure 3.10 (a)** Core wrapped in Teflon tape before ageing **(b)** Core placed in ageing cell **(c)** Unwrapped core ready for oil recovery test ..... 32
**Figure 3.11** Illustration of the SI set-up (Khan et al., 2023) ..... 33
**Figure 3.12** Core SK 1 wrapped in aluminum tape before high pressure FI oil recovery test ..... 34
**Figure 3.13** Illustration of high-pressure FI set-up ..... 35
**Figure 3.14** Illustration of low-pressure FI set-up. Modified from (Khan et al., 2023) ..... 35
**Figure 4.1** Oil recovery through FI of SK1 with FW-injection in secondary mode and CFW-injection in tertiary mode at high pressure. Test conducted at T=70℃ and P=50 bars. ..... 37
**Figure 4.2** Illustration of SK1 (a) Before FI (b) After high pressure FI ..... 38
**Figure 4.3** Oil recovery and pressure drop through FI of SK2 with FW-injection in secondary mode and CFW-injection in tertiary mode. Test conducted at T=70℃ and P=10 bars. ..... 39
**Figure 4.4** Oil recovery and pressure drop through FI of SK3 with CFW-injection in secondary mode and SW-injection in tertiary mode. Test conducted at T=70℃ and P=10 bars. ..... 40
**Figure 4.5** Oil recovery through SI of SK4 with FW. Test conducted at T=70℃ and P=10 bars. ..... 41
**Figure 4.6** Oil recovery of SK5 through SI with FW. Test conducted at T=70℃ and P=10 bars. ..... 41
**Figure 4.7** Oil recovery and pressure drop after SI through FI of SK4 with CFW-injection in secondary mode. Test conducted at T=70℃ and P=10 bars. ..... 42
**Figure 4.8** Oil recovery and pressure drop after SI through FI of SK5 with FW-injection in secondary mode and CFW-injection in tertiary mode. Test conducted at T=70℃ and P=10 bars. ..... 43

**Figure 4.9 (a)** SI into oil (AN=0.58 mg of KOH/g) at 110℃ and P=10 bars (Khan et al., 2023) (**b)** SI into oil (AN=1.80 mg of KOH/g) at 70℃ and P= 10 bars (SK5)..... 45
**Figure 4.10** SI experiment conducted by Fathi et al. (2010) at T=110℃ illustrating recovery factor of ..... **(a)** Oil T.O (AN=1.5 mg of KOH/g) and **(b)** Oil O.O (AN=1.8 mg of KOH/g) ..... 45
**Figure 4.11** Temperature and AN effect on oil recovery at P=10 bars. Comparison of **(a)** FI in oil (AN=0.58 mgKOH/g) at T=130℃ (Khan et al., 2023) **(b)** FI in oil (AN=1.80 mgKOH/g) at T=70℃ (SK2) ..... 46
**Figure 4.12** Pressure effect on oil recovery at T=70 ℃. Comparison of injection pressure at **(a)** P=50 bars (SK1) and **(b)** P=10 bars (SK2) ..... 47
**Figure 4.13 (a)** SK1 after high pressure FI test **(b)** SK2 after low pressure FI test..... 48
**Figure 4.14** Injection mode effect on oil recovery. Tests conducted at T=70℃ and P=10 bars. Comparison of CFW-injection in **(a)** secondary mode (SK3) **(b)** tertiary mode (SK2)..... 49
**Figure 4.15** Tests conducted at T=70℃ and P=10 bars. FI with CFW injection in secondary mode **(a)** without SI (SK3) **(b)** after SI (SK4) ..... 50
**Figure 4.16** Tests conducted at T=70℃ and P=10 bars. FI with CFW injection in tertiary mode **(a)** without SI (SK2) **(b)** after SI (SK5) ..... 51
**Figure 4.17** FI injection mode effect on oil recovery after SI. Tests conducted at T=70℃ and P=10 bars. Comparison of CFW-injection in **(a)** secondary mode (SK4) **(b)** tertiary mode (SK5) ..... 52

# List of tables

**Table 2.1** Classification of emerging EOR processes (Piñerez Torrijos, 2017) ..... 4
**Table 2.2** Method of displacement and steps for the Amott test ..... 9
**Table 2.3** Wettability classification based on Amott-Harvey index range ..... 10
**Table 3.1** Physical properties of the Stevns Klint cores used for the experiments ..... 22
**Table 3.2** Physical properties of Heidrun base oil and RES-40 test oil ..... 23
**Table 3.3** Composition of ions and physical properties of the brines ..... 23
**Table 3.4** Injection strategies involving SI and FI ..... 36
**Table 4.1** Summary of the results from all the injection strategies ..... 44
**Table A.1** 1st test. High pressure FI by FW CFW (SK1) ..... 60
**Table A.2** 2nd test. Low pressure FI by FW CFW (SK2) ..... 61
**Table A.3** 3rd test. Low pressure FI by CFW SW (SK3) ..... 62
**Table A.4** 4th test. Spontaneous imbibition by FW (SK4) ..... 63
**Table A.5** 5th test. Spontaneous imbibition by FW (SK5) ..... 63
**Table A.6** 6th test. Low pressure FI by CFW after SI (SK4) ..... 64
**Table A.7** 7th test. Low pressure FI by FW CFW after SI (SK5) ..... 65

**Abbreviations**

| | |
|---|---|
| AN | Acid number |
| CCUS | Carbon, Capture, Utilization, Storage |
| CFW | Carbonated formation water |
| CW | Carbonated water |
| CWI | Carbonated water injection |
| dP | Differential pressure |
| E | Total displacement efficiency |
| $E_D$ | Microscopic displacement efficiency |
| $E_V$ | Macroscopic displacement efficiency |
| EOR | Enhanced oil recovery |
| FD | Forced displacement |
| FI | Forced imbibition |
| FW | Formation water |
| IFT | Interfacial tension |
| M | Mobility ratio |
| OOIP | Original oil in place |
| PV | Pore volume |
| SD | Spontaneous displacement |
| SI | Spontaneous imbibition |
| SW | Sea water |
| VB0S | Vallhall brine zero sulfate |
| VF | Viscous flooding |
| WBT | Water breakthrough |

# 1. Introduction

The Paris agreement set a goal for net zero emissions by 2050, with a global warming of no more than 1.5℃. Simultaneously, the world is witnessing a continual rise in energy demand, driven by population growth and industrialization of developing countries. Petroleum industry plays a big part in meeting these demands. However, it faces challenges when it comes to environmental impact, sustainability, and depletion of oil reserves. Many petroleum reserves today are in their mature stage, where oil and gas are not easily accessible. Enhanced oil recovery (EOR) techniques are important for utilizing the full potential of these mature reserves, while reducing the need for exploring and developing new fields, thereby minimizing environmental impact.

Around 60 percent of the global oil production can be attributed to carbonate reservoirs (Bagrintseva, 2015). The oil recovery factor in carbonate reservoirs is significantly lower compared to that of sandstone reservoirs, with average estimation falling below 35 %OOIP (Sheng, 2013). Research on EOR techniques holds special relevance for carbonate reservoirs due to the natural characteristics of these reservoirs being lower oil recovery, limited fluid mobility, reservoir heterogeneity, and the presence of trapped oil.

The use of carbon dioxide ($CO_2$) for EOR can be effective, not only for increasing the ultimate recovery from mature reserves, but also for carbon sequestration. $CO_2$ is then injected inside the reservoir to displace the residual oil. By combining carbon sequestration and EOR, this is considered as an environmental alternative for utilizing the reservoir potential. It is an EOR technique that also faces some challenges, especially for heterogenous reservoirs like carbonates. Problems can occur due to poor mobility ratio, as $CO_2$ has a much lower viscosity than oil, which can lead to viscous fingering and early $CO_2$ breakthrough (Al-Shargabi et al., 2022).

Carbonated water injection (CWI) is an emerging EOR technique that serves as an alternative to traditional $CO_2$ injection. In CWI, $CO_2$ is dissolved in water prior to injection into the reservoir. It is a technique that shows great promise for increasing oil recovery in depleted reserves, as it addresses some of the challenges that are faced in pure $CO_2$ injection, mainly poor sweep efficiency and separation due to gravity (Bisweswar et al., 2020). CWI is also a safer technique for carbon storage, as the $CO_2$ is dissolved in water and oil, instead of existing in a free phase (Riazi et al., 2009).

There are several studies done on CWI, and multiple oil recovery mechanisms have been suggested. Sohrabi et al. (2009) conducted a CWI experiment on two oils with large difference in viscosity. From this experiment two main oil recovery mechanisms were observed: swelling and mobilization of trapped oil and reduction of oil viscosity. These are both direct consequences of the $CO_2$ from the carbonated water (CW) dissolving into the oil phase and changing the properties of the oil.

Drexler et al. (2020) conducted a CWI study on carbonate rocks were the wettability was measured by contact angle before and after CWI of the carbonates. Results from this study

concluded that the dissolution of $CO_2$ altered the wettability of the carbonate core samples from mixed-wet to water-wet. This mechanism is also observed in numerous other studies (Ruidiaz et al., 2018; Seyyedi et al., 2015). The reason for this wettability alteration is because $CO_2$ reduces the pH in the injected water, affecting the electrical charges on the interface of water and rock, causing an increased affinity towards water on the surface. So, decreasing the acid number (AN) will alter the wettability towards a more water-wet system. It is an important mechanism, especially for carbonate reservoirs, as they tend to be naturally mixed-wet or even slightly oil-wet. Strongly water-wet systems are preferred in reservoirs as this gives the best displacement efficiency.

The effect of traditional oil recovery mechanisms involved in carbonated formation water (CFW) injection in chalk reservoirs will be examined during this thesis. Various injection strategies are tested to answer the objectives as presented.

## 1.1 Objectives

The primary objective of this study is to assess the oil recovery potential of the Stevns Klint chalk core samples, which exhibits similar properties to the North Sea chalk reservoirs, particularity the Ekofisk field. It involves using CFW as injection fluid for enhanced oil recovery (EOR). Several methods are evaluated to get a better understanding of the most ideal oil recovery strategies:

- The effect of the injection mode is to be evaluated. Injection fluids in this study include sea water (SW), formation water (FW), and CFW. Forced imbibition (FI) using CFW injection in secondary and tertiary mode is compared. Oil recovery and amount of water injected will be discussed for both injection modes.
- Different injection pressures are also going to be evaluated. The strategies to be assessed include FI using CFW under high- and low-pressure conditions. This is done to check if the amount of $CO_2$ dissolved in the water has any effect on the total recovery.
- Temperature effect on oil recovery is evaluated by comparing the results from similar experiments conducted at high temperature, as this study is done at low temperature.
- The wettability conditions of the cores are also being assessed through spontaneous imbibition (SI) experiments with FW. Results from different types of oils with different AN and wettability are to be compared with this study. Both to see the effect of AN on wettability but also to see the wettability effect on total oil recovery.

The trends of the different strategies will be discussed. Including the water breakthrough (WBT) point, volume of water injected, recovery of %OOIP, and the differential pressure (dP). By addressing these objectives, this study aims to enhance the understanding of oil recovery mechanisms in chalk using CFW at different injection strategies.

# 2. Theory and fundamentals

## 2.1 Oil recovery mechanism

Oil recovery mechanisms are divided into three stages: primary, secondary, and tertiary stage. The primary stage represents the initial stage of oil recovery where only the natural forces in the reservoir are responsible for the production. Tertiary stage, also referred to as enhanced oil recovery, represents the last stage of oil recovery (Green & Willhite, 2018a).

### 2.1.1 Primary stage

This is the initial stage of oil recovery, during which oil is produced through natural reservoir forces. Oil flows naturally from the reservoir to the surface due to the pressure difference, so fluid injection is not needed during this stage. In essence, there exist six different fundamental mechanisms that facilitate the natural energy required for oil recovery: depletion drive, water drive, gravity drainage drive, rock and liquid expansion drive, gas cap drive, and finally combination drive (Tarek & Meehan, 2012). Oil recovery is usually below 30% during this stage (Kokal & Al-Kaabi, 2010).

### 2.1.2 Secondary stage

Following the initial discovery and primary stage, conventional oil reserves tend to experience a loss of their drive mechanism that was responsible for the original oil extraction (Alagorni et al., 2015). Secondary recovery is defined as any oil production from artificial energy in the reservoir, which includes pressure maintenance through gas, water or WAG injection (Tarek & Meehan, 2012). The recovery rate during this stage usually lies within 30-50% (Kokal & Al-Kaabi, 2010).

### 2.1.3 Tertiary stage (enhanced oil recovery)

When the production of oil is plateauing or becomes economically unviable after secondary recovery, a tertiary process, EOR, is employed to displace additional oil. The external forces in the tertiary process involve the use of gases, chemicals, thermal energy, and/or other processes for oil displacement. The term “enhanced oil recovery” is now more commonly used instead of “tertiary recovery”, as the latter suggests that external forces must always be employed after primary and secondary recovery, which is not always the case. For reservoirs that contain heavy crude oil with high viscosity, it may not flow at rates that are economically viable under natural energy drives. In such reservoirs, the utilization of thermal energy may be the only option to recover a substantial amount of oil. A method typically considered a tertiary process would then be employed as the initial and final stage of oil recovery (Green & Willhite, 2018a). Figure 2.1 illustrates the different stages of oil recovery and their respected recovery factors.

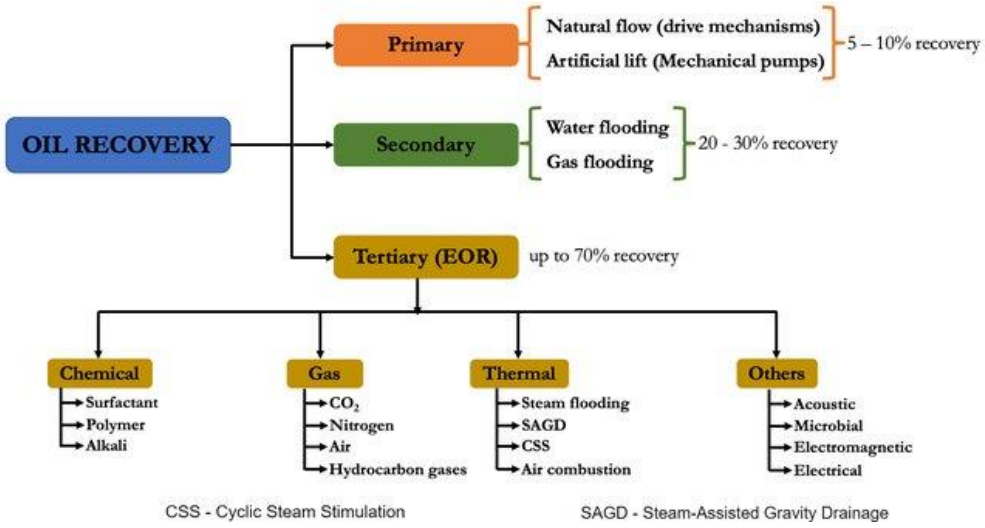


**Figure 2.1** Stages of oil recovery and related recovery factor (Bello et al., 2023)

Thermal energy for EOR generally involves the use of hot water/steam, or oil combustion in-situ. Heat lowers the viscosity, making oil recovery easier, especially for heavy crude oils.

Gas injection is another traditional EOR process utilized. Typically, nitrogen, hydrocarbon gases, flue gases, and $CO_2$ are injected into the reservoir to displace oil. Hydrocarbon gases, $CO_2$, and flue gases are miscible in oil and can therefore form a single phase. This changes the composition of the oil, reducing the viscosity and density, and consequently increasing the mobility.

Chemical EOR techniques involve injecting specific chemicals, such as surfactants/polymers or alkaline agents, to leverage a combination of phase behavior and interfacial tension reduction to displace oil and enhance recovery.

Beyond these traditional EOR processes there has been development into newer methods. Examples of emerging EOR processes are classified in table 2.1.

**Table 2.1** Classification of emerging EOR processes (Piñerez Torrijos, 2017)

| Emerging EOR process |
|---|
| Smart water |
| Carbonated water |
| Microbial EOR |
| Enzymatic EOR |
| Electromagnetic heating |
| Surface mining and extraction |
| Nano particles |

## 2.2 Reservoir rock

Reservoir rocks can be classified into two types (Satter et al., 2008a):

- **Clastic rocks**: This category includes sands, sandstones, conglomerates, and to a lesser extent, siltstones, and shale. They are created by the processes of erosion, transformation, and deposition acting upon preexisting rocks.
- **Carbonate rocks**: This category includes dolomites, reef rocks, limestones, and chalk. They are the result of organic matter and chemical sediment.

Oil recovery is heavily dependent on the reservoir rock, or more specifically the structure of the rock. Porosity and permeability of the reservoir are two parameters that influence the recovery and will therefore be presented in this subchapter.

### 2.2.1 Porosity

Porosity is a measurement of the pore volume of the rock, which decides how much fluid potentially can be stored inside. Only two parameters affect the absolute porosity, the pore vs bulk volume, usually presented in percentage. Equation 2.1 shows the formula for calculating the total porosity.

$$\phi = \frac{V_P}{V_T} * 100\% \qquad 2.1$$

$\phi$ – Absolute porosity, %
$V_P$ – Pore volume, mL
$V_T$ – Total volume, mL

High total porosity is desirable, but it includes pore spaces that both are interconnected and isolated. The pores that are not interconnected in the reservoir do not contribute to the production of oil. It is therefore normal to differentiate between absolute and effective porosity. Effective porosity is the portion that allows for fluid flow, and only includes the interconnected pores, and is therefore of more interest to reservoir engineers (Satter et al., 2008a).

### 2.2.2 Permeability

Permeability refers to a rock's ability to allow fluid flow under a driving force, either natural or artificial (Sanni, 2018; Satter et al., 2008a). Several different factors influence the permeability, including the rock size, shape, configuration, and pore space connectivity.

Generally, it is divided into absolute, effective, and relative permeability. Absolute permeability refers to the permeability of the rock when it is completely saturated with a single fluid phase. Effective permeability is the permeability of a specific fluid when other fluids are present in the rock, for example water and oil. Relative permeability refers to the ratio of effective permeability to absolute permeability.

Darcy's law is based on the empirical observation of Henry Darcy in 1856 but can be derived from the Navier Stokes equation for incompressible fluid (Sanni, 2018). This law allows us to calculate the absolute permeability, and is expressed as follows:

$$k = \frac{q*\mu*L}{A*\Delta p} \qquad 2.2$$

k – permeability, $m^2$
q – flow rate, $m^3/s$
L – length of core, m
A – cross-sectional area, $m^2$
Δp – differential pressure, Pa

It is important to note that equation 2.2 should only be used as an estimation of the permeability of core samples, since it comes with several conditions that are difficult to meet. These reads as follows (Satter et al., 2008a):

1. Fluid is incompressible.
2. Flow is in a steady state.
3. Fluid flow is in the horizontal direction.
4. Flow is laminar, without any turbulence effects.
5. Only one fluid is present in the pore space.
6. No chemical reaction between the rock and the fluid.

## 2.3 Mineralogy of carbonates

Currently, around 60% of the global oil production can be attributed to reservoir rocks formed from carbonates (Bagrintseva, 2015). Understanding the mineralogy of these rocks is important due to their complex nature, contributed from diverse compositions, crystal structures, and formation processes.

Carbonates are composed of $CO_3^{2-}$ along with one or more cations, mainly $Ca^{2+}$ , $Mg^{2+}$, $Fe^{2+}$, $Mn^{2+}$, $Zn^{2+}$, $Ba^{2+}$, $Sr^{2+}$, and $Cu^{2+}$ (Ahr, 2008; Bjorlykke, 2010b). If the majority of the rock is containing carbonate minerals it is generally classified as a carbonate rock (Mazzullo et al., 1992). Calcite ($CaCO_3$) and dolomites ($CaMg(CO_3)_2$) are the two predominant carbonates sediments in the world, formed from the cations $Ca^{2+}$ and $Mg^{2+}$. Sedimentation of carbonates is directly influenced by the transportation of these cations from river systems into the ocean. As carbonates are typically formed in shallow, warm oceanic environments (Lucia, 2007).

Chalk is a type of carbonate rock that is of special importance in the North Sea oil reservoirs. They are made of almost pure calcite. The chalk reservoirs, like the Ekofisk field, is characterized by high porosity and low permeability (Bjorlykke, 2010a). The natural fracturing of these types of reservoirs determines the effective permeability.

## 2.4 Wettability

Wettability is the ability of a fluid to either spread or adhere to a solid surface when other immiscible fluids are present. It is a measure of how well a fluid wets or contacts the reservoir rock. It is an important parameter that influences the fluid flow and efficiency of oil recovery operations. Wettability influences the distribution of fluids within the pores. The wetting fluid phase fills up the narrow pores, while the non-wetting fluid tends to fill the open channels (Ahmed, 2019).

In the context of the oil reservoir, wettability is typically divided into three different phases:

- Oil-wet: The reservoir rock prefers oil over water in an oil-wet scenario. Oil will adhere to the solid surface, forming a continuous coating in the pores. During this, a significant portion of the oil may be trapped in the smaller pore spaces.
- Water-wet: A favorable wetting phase when it comes to oil recovery. In a water-wet scenario, the rock surface prefers water over oil. The water forms a continuous coating on the surface, reducing the possibility of oil getting trapped in narrow spaces. The water will in this scenario occupy the narrow passages, leading to higher oil recovery.
- Mixed-wet: In a mixed-wet scenario the reservoir exhibits traits from both water-wet and oil-wet systems. The rock surface will in these scenarios both have an affinity towards water and oil. Other parameters like mineralogy, fluid- and rock composition may determine the wetting preferences during intermediate-wet scenarios.

All the wettability phases are illustrated in figure 2.2.

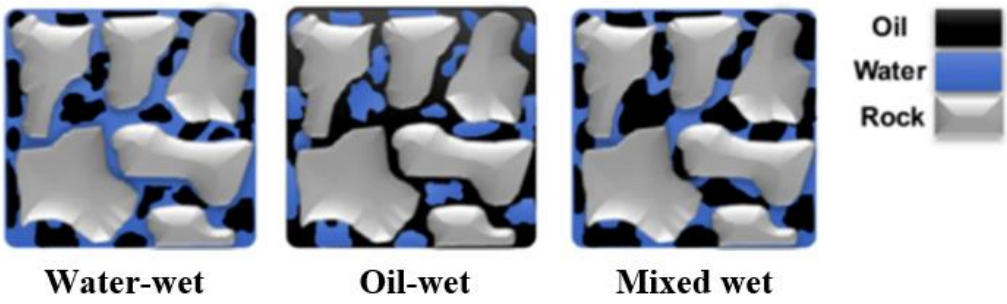


**Figure 2.2** Illustration of water-wet, oil-wet, and mixed-wet system in a porous media (Mousavi Moghadam & Salehi, 2019)

As mentioned, the wettability of the reservoir can determine the amount of entrapped oil and is therefore a very important parameter when it comes to enhancing oil recovery. EOR methods will look towards methods of changing the wettability towards a more water-wet side.

Carbonate reservoirs generally tends to favor mixed-wet or slightly oil-wet conditions, as it promotes the adsorption of oil onto the surface (Sagbana et al., 2022; Yao et al., 2021). A considerable amount of oil therefore remains in the reservoir after the primary and secondary stages. Hence, modifying the wettability conditions during the tertiary stage is essential to fully exploit the reservoir potential.

## 2.5 Methods for determining wettability

Measuring wettability is crucial for understanding fluid behavior, optimizing production, and improving oil recovery. This makes it possible to make more informed decisions during the lifecycle of the reservoir. There are several different ways of measuring wettability. Certain techniques are more suited for analyzing specific surface areas, while others are more appropriate for studying complex, porous media. The most used popular approaches will be discussed in this subchapter.

### 2.5.1 Contact angle

Contact angle measures the wettability of a specific, flat, and smooth surface. An oil drop is placed on the surface and the angle is measured. It is important to note that contact angle measurement does not take the roughness, heterogeneity, and complexity of the reservoirs into account. It can measure completely different wettability conditions depending on what area of the rock is being measured and should therefore only be used as representation of wettability of artificial cores at laboratory scale, and not for real-life reservoir conditions. Figure 2.3 showcases how wettability is determined by the contact angle of the oil droplets.

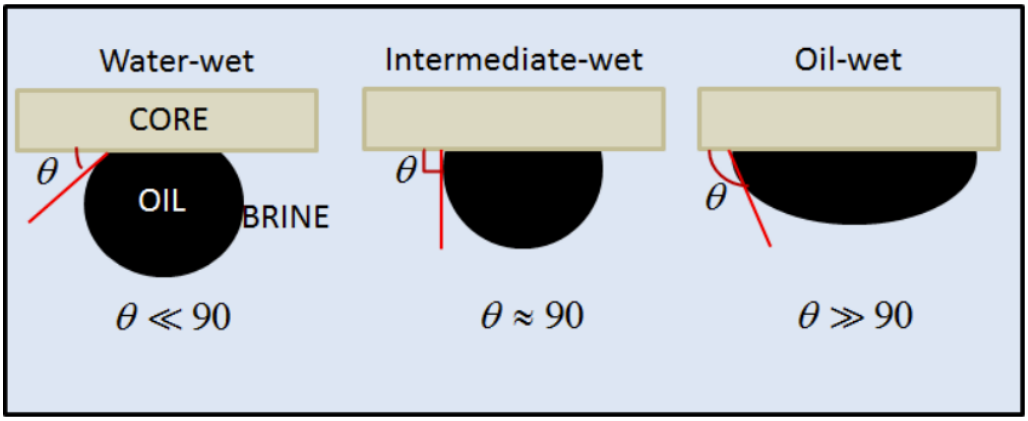


**Figure 2.3** Illustration of the different wettability conditions in an oil reservoir (Teklu et al., 2015)

The angles of the droplet determines the wettability condition of the specific surface (Dandekar, 2013). Contact angles ranging between 0-75° suggests a water-wet system, and the lower the angle the more strongly the surface preference is towards water. Contact angles between 105-180° suggest an oil-wet system, and the higher the angle the more strongly the surface preference is towards oil. A contact angle between 75-105° suggests a neutrally wet system.

### 2.5.2 Spontaneous imbibition

A simple way of measuring wettability across an entire core is to introduce it to SI. The process of SI involves the displacement of a nonwetting fluid by a wetting fluid solely through capillary action, and require no additional equipment (Morrow & Mason, 2001). A core saturated with oil is placed in a cell holder filled with water brine.

By performing SI, we can observe the wetting conditions within the pore spaces. The recovery rate during this test is directly correlated to the wettability condition. A strong water-wet core sample will experience a higher and faster oil recovery rate during SI, while low oil recovery rate suggests a weak water-wet system.

The system is mixed-wet or oil-wet in cases when there is no oil recovery during SI with water as imbibing fluid. For instances where there is no production of oil by SI it is possible to measure how strongly oil-wet the systems are. Water is then displaced by oil, and the water production is recorded. A higher water recovery rate would then suggest that the system is strongly oil wet.

### 2.5.3 Amott-Harvey

The Amott test is the most used for core samples and is suited for measuring the wettability of reservoir rocks. This presents the average wettability throughout the porous media, instead of just specific surface areas. The test consists of a combination of forced and spontaneous displacement (FD and SD). During this test, the term displacement is used instead of imbibition, as imbibition describes the displacement of the nonwetting phase. Since both the non-wetting and wetting fluid is going through the process, coupled with the fact that we do not know the wetting fluid phase before starting the test, it is more accurate to use the term displacement (Dandekar, 2013). The test is carried out by four displacement operations as shown in table 2.2 (Amott, 1959).

**Table 2.2** Method of displacement and steps for the Amott test

| | **Step 1** | **Step 2** | **Step 3** | **Step 4** |
|---|---|---|---|---|
| **Method of displacement** | Water is displaced by oil through SD | Water is displaced by oil through FD | Oil is displaced by water through SD | Oil is displaced by water through FD |

Measurement of wettability is obtained by comparing the volume from spontaneous displacement to total displacement. The different ratios can be determined using equations 2.3-2.6 presented below (Dandekar, 2013):

$$\delta_o = \frac{V_{ws}}{V_{wt}} \quad 2.3$$

$$\delta_w = \frac{V_{os}}{V_{ot}} \quad 2.4$$

$$V_{wt} = V_{ws} + V_{wf} \quad 2.5$$

$$V_{ot} = V_{os} + V_{of} \quad 2.6$$

$V_{os}$ – Volume of spontaneously displaced oil [ml]

$V_{wf}$ – Volume of water released by forced displacement [ml]
$V_{of}$ – Volume of oil released by forced displacement [ml]
$V_{wt}$ – Volume of total displaced water [ml]
$V_{ot}$ – Volume of total displaced oil [ml]

From these equations the Amott-Harvey wettability index, $I_{AH}$, can be calculated as follows:

$$I_{AH} = \delta_w - \delta_o \qquad 2.7$$

The wettability condition of the core is decided based on the index presented in equation 2.7. Classification based on the Amott-Harvey wettability index values are presented in table 2.3 (Dandekar, 2013).

**Table 2.3** Wettability classification based on Amott-Harvey index range

| $I_{AH}$ | **Wettability** |
|---|---|
| +0.3 to +1.0 | Water-wet |
| +0.1 to +0.3 | Weak water-wet |
| -0.1 to +0.1 | Mixed-wet |
| -0.3 to -0.1 | Weak oil-wet |
| -1.0 to -0.3 | Oil wet |

Figure 2.4 illustrates steps 1 and 3 (SD) for the Amott test, defined in table 2.2.

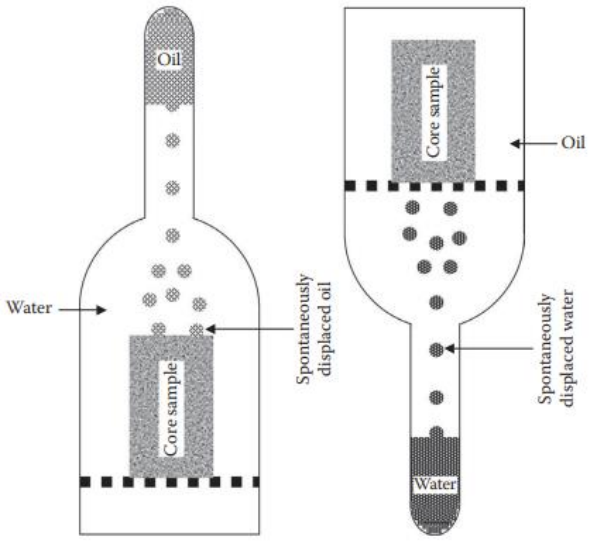


**Figure 2.4** Example of spontaneous displacement of oil and water for Amott test (Dandekar, 2013)

### 2.5.4 USBM

Another widely used technique for measuring wettability is the United States of Mines, USBM, method developed by Donaldson et al. (1969). As for the Amott test, it measures the average wettability of a core sample. Contrary to the Amott test, USBM only involves the process of forced displacement. The USBM method utilizes a centrifuge set-up for measuring the wettability, as illustrated in figure 2.5.

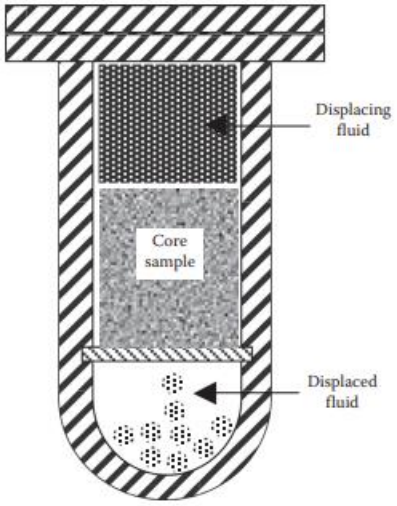


**Figure 2.5** Centrifuge set-up for USBM test (Dandekar, 2013)

Irreducible water saturation, $S_{wi}$, is established in the core by subjecting the water-saturated core sample to high-speed centrifugation under the presence of displacing oil phase. When the water production reaches a plateau, centrifugation is stopped, and irreducible water saturation is calculated. The core is then placed in brine and by centrifugation this brine is forcibly displacing oil. Centrifugation speed is then increased stepwise until capillary pressure of -10 psi, during which effective pressure and water saturation are measured at every step, and average water saturation is calculated by the quantity of oil displacement. This process is then reversed, and oil is displacing the brine, until capillary pressure of +10 psi is reached (Dandekar, 2013).

When this is done, the capillary pressure is plotted against water saturation. The USBM wettability index is then determined from the ratio of the area under the two capillary pressure curves, formulated as:

$$I_{USBM} = log\left[\frac{A_o}{A_b}\right] \qquad 2.8$$

$I_{USBM}$ – USBM wettability index
$A_o$ – Area of the oil curve
$A_b$ – Area of the brine curve

$I_{USBM} > 0$ suggests a water-wet system, $I_{USBM} < 0$ suggests an oil-wet system, and $I_{USBM} \approx 0$ suggests a mixed-wet system. The curves of a water-wet and oil-wet system based on the wettability index are shown in figure 2.6.

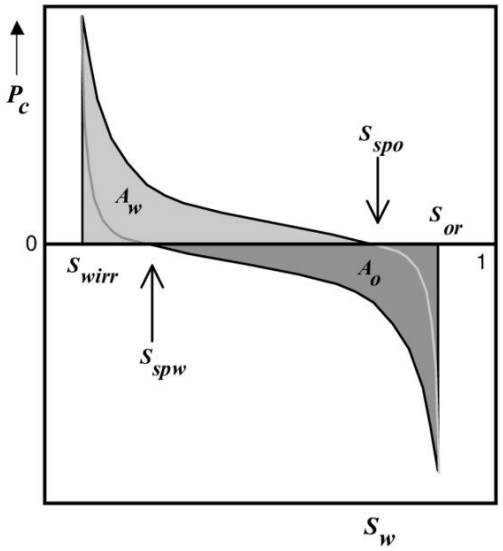


**Figure 2.6** Plot of capillary pressure against water saturation used for wettability index (Reed et al., 2014)

## 2.6 Displacement forces

When talking about displacement forces it is normal to separate into microscopic and macroscopic scales. Microscopic displacement refers to the displacement of fluids at the pore scale. Parameters that play significant roles at microscopic scales include capillary forces, viscous force, interfacial tension, and wettability. While gravity forces, and reservoir heterogeneity place significant roles at the macroscopic scale.

### 2.6.1 Displacement efficiency

Displacement efficiency is a measurement of the proportion of fluid in a porous medium that can be effectively mobilized by a displacement process, such as oil displacement by water in a reservoir (Fanchi & Christiansen, 2016a). The total displacement efficiency is the product of both the microscopic and macroscopic forces acting upon the reservoir. This is formulated as follows (Green & Willhite, 2018a):

$$E = E_V E_D \qquad 2.9$$

E – Total displacement efficiency
$E_V$ – Volumetric sweep/macroscopic displacement efficiency
$E_D$ – Microscopic displacement efficiency

The parameters are expressed as fractions between zero and one, so for an effective displacement the value of total displacement efficiency, E, should be close to one.

Microscopic displacement efficiency, $E_D$, relates to the amount of oil that is extracted from the pores and can be formulated like this:

$$E_D = \frac{S_{oi} - S_{or}}{S_{oi}} \quad 2.10$$

$S_{oi}$ – Initial oil saturation
$S_{or}$ – Residual oil saturation

So, to get an effective microscopic displacement one must look to reduce the residual oil saturation.

The macroscopic displacement efficiency, $E_v$, is a product of the areal and vertical sweep efficiency (Green & Willhite, 2018c):

$$E_V = E_A E_i \quad 2.11$$

$E_A$ – Areal sweep
$E_i$ – Vertical sweep

Combining these equations gives us a formula for the total displacement efficiency:

$$E = (E_A E_i) * \frac{S_{oi} - S_{or}}{S_{oi}} \quad 2.12$$

Every parameter is formulated in fractions between zero and one. By looking at equation 2.x one can see that for ideal displacement efficiency it is beneficial to have the areal and vertical sweep close to one. For the microscopic scale the goal is to reduce residual oil in the pores close to zero, with the help of optimum EOR methods for displacement.

### 2.6.2 Fluid mobility through porous media

An important concept in oil recovery is mobility, as it affects the efficiency of displacement. The mobility of a fluid is defined as its ability to flow through a porous medium under differential pressure, and it is dependent on the viscosity of the displaced fluid and the rock permeability. Mobility can be formulated as follows (Fanchi, 2010):

$$\lambda_x = \frac{k_x}{\mu_x} \quad 2.13$$

$\lambda_x$ – Mobility of fluid x
$k_x$ – Effective permeability to fluid x
$\mu_x$ – Viscosity of fluid x

x – subscript denoting fluid phase (water, gas, or oil)

An oil reservoir generally experiences multiphase flow, where the mobility of displaced fluid is affected by the presence of other fluids such as water, which leads to the concept of mobility ratio. This is the ratio of the mobility of displacing fluid to the mobility of the displaced fluid. An example of this is the mobility ratio of water to oil, during a waterflood scenario:

$$M_{w,o} = \frac{\lambda_w}{\lambda_o} = \frac{k_{rw}(S_{or})/\mu_w}{k_{ro}(S_{wc})/\mu_o} \qquad 2.14$$

$M_{w,o}$ – Mobility ratio, water to oil
$\lambda_w$ – Mobility of displacing fluid, water
$\lambda_o$ – Mobility of displaced fluid, oil
$k_{rw}$ – Relative permeability of water
$k_{ro}$ – Relative permeability of oil
$S_{wc}$ – Connate water saturation
$S_{or}$ – Residual oil saturation
$\mu_w$ – Viscosity of water
$\mu_o$ – Viscosity of oil

When the mobility ratio is less than 1, the displacing fluid works more efficiently, leading to higher recovery. Conversely, a mobility ratio of more than 1 is considered unfavorable. When the mobility ratio is too high the reservoir may experience a phenomenon called viscous fingering. By looking at equation 2.8 one can see that this happens when the displacing fluid has too high viscosity, hence the name viscous fingering.

Figure 2.7 (a) shows an example of viscous fingering during a waterflood with mobility ratio of more than 1. Figure 2.7 (b) is an example of polymers being added to increase the viscosity of the displacing fluid and thereby lowering the mobility ratio to 1 or less, creating a stable front.

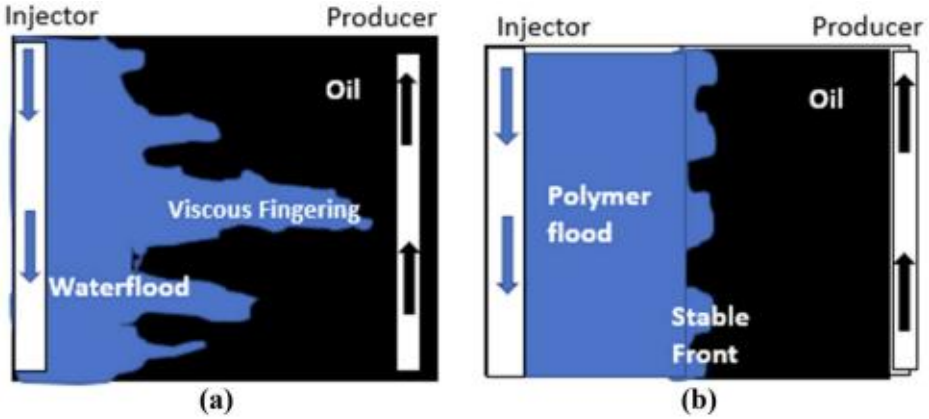


**Figure 2.7 (a)** Waterflood with M>1 **(b)** Polymer flood at M≤1 (Gbadamosi et al., 2019)

### 2.6.3 Gravity forces

Gravity drainage, also referred to as gravity displacement force, is an important factor in fluid flow within a reservoir. The fluid with the higher density displaces a lighter fluid due to the influence of gravity. When placing a jar with water and oil, the denser fluid (water) will rest at the bottom while the less dense fluid (oil) will rest at the top, due to the gravity force (Tarek & Meehan, 2012). The hydrostatic pressure difference between oil and water from the gravity force can be formulated like this:

$$\Delta P_g = \Delta \rho g Z \qquad 2.15$$

$\Delta P_g$ – Hydrostatic pressure difference between fluid phases due to gravity [Pa]
$\Delta \rho$ – Difference in density between fluid phases $[kg/m^3]$
g – Gravity constant $[9.81\ m/s^2]$
Z – Vertical depth [m]

### 2.6.4 Viscous forces

Viscous forces play a fundamental role in fluid behavior and displacement efficiency. During a waterflood injection it has been proven that the viscous forces can be even more influential than gravity forces if the viscosity and injection rates are high enough (Satter et al., 2008c).

The influence of viscous forces in a porous media can be observed through the value of pressure drop that arises when a fluid flows through the medium. An approach to calculating the effect of viscosity is to consider the medium as a collection of capillary tubes. The pressure drop can then be calculated through Poiseuille's law, assuming laminar flow (Craft & Hawkins, 2015a; Green & Willhite, 2018b):

$$\Delta p = -\frac{8\mu L \bar{v}}{r^2 g_c} \qquad 2.16$$

$\Delta p$ – pressure drop across the tube (Pa)

L – Length of the tube (m)
r – Tube radius (m)
$\bar{v}$ – Average tube velocity (m/s)
$g_c$ – Gravity conversion factor
$\mu$ – Viscosity of flowing fluid (Pa*s)

### 2.6.5 Capillary force

Capillary pressure is a fundamental property that governs the behavior of fluids in multiphase flow within porous media (Lake, 2010). It represents the pressure difference across the interface between two immiscible fluids (oil and water), or conversely, between the non-wetting phase and the wetting phase. This is expressed as:

$$P_{NW} - P_W = \frac{2\sigma cos\theta}{R} = P_c \quad 2.17$$

$P_c$ – Capillary pressure [Pa]
$P_{NW}$ – Pressure of non-wetting fluid phase [Pa]
$P_W$ – Pressure of wetting fluid phase [Pa]
$\sigma$ – Interfacial tension (IFT) between the two fluid phases [N/m]
$\theta$ – Contact angle [°]
R – Pore radius [m]

As illustrated in equation 2.9, the IFT and capillary pressure are directly proportional. Pressure from the non-wetting fluid phase is higher than the wetting fluid phase, so for this equation the capillary pressure will always be a positive number. Both oil and water can be in the wetting fluid phase, depending on the pressure relation.

Capillary forces can both be favorable and unfavorable for oil displacement. For fractured reservoirs capillary forces act as an important oil recovery mechanism. However, for non-fractured reservoirs, capillary forces can cause trapping of oil in the pores, and consequently increase the residual oil saturation.

### 2.6.6 Capillary number

All the displacement forces interact with each other, and it is therefore relevant to describe the relation between these forces. The impact of viscous forces and interfacial tension on residual oil entrapment and mobility has been studied extensively over the years. Thus, a correlation between this relation and the oil recovery fraction has been made. Capillary number, $N_c$, is a dimensionless parameter that describes the relation between viscous and capillary forces and is formulated as follows (Craft & Hawkins, 2015b):

$$N_c = \frac{v_o \mu_w}{\sigma_{ow}} = \frac{k_o \Delta p}{\phi \sigma_{ow} L} \quad 2.18$$

$N_c$ – Capillary number [Dimensionless]
$v_o$ – Velocity [m/s]
$\mu_w$ – Viscosity of displacing fluid (water) [Pa*s]
$\sigma_{ow}$ – Interfacial tension between displaced and displacing fluid (oil and water) [N/m]
$k_o$ – Effective permeability of the displaced fluid (oil) [$m^2$]
$\frac{\Delta p}{L}$ – Differential pressure related to flow [Pa/m]
$\phi$ – Porosity [Dimensionless]

The capillary number increases proportionally with the viscosity of displacing fluid and decreases proportionally with the capillary pressure. Figure 2.7 is a great illustration of the capillary number effect on the residual oil saturation. From this illustration one can conclude

that capillary numbers above $10^{-5}$ are necessary for mobilizing the oil and enhancing the oil recovery.

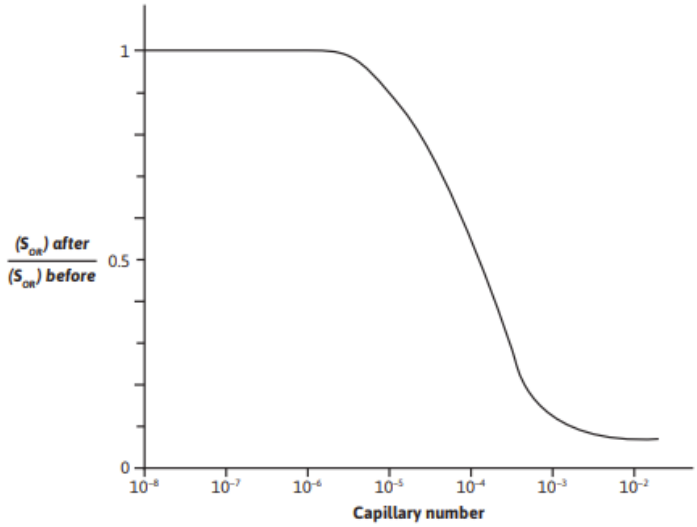


**Figure 2.8** Capillary number and relation to residual oil (Craft & Hawkins, 2015b)

## 2.7 EOR in carbonates

Enhanced oil recovery methods are employed to extract additional oil from the reservoirs beyond the primary and secondary recovery stages. Carbonate reservoirs are mainly made of limestones and dolomites (Satter et al., 2008a). They range from soft to chalky, cavernous, or vuggy, which presents some unique challenges and opportunities for EOR due to their complex pore structures and varying rock properties. Thermal, chemical, and gas methods can all be utilized as EOR techniques in carbonate reservoirs.

It is important to note that although thermal methods are a potential EOR method, this is yet to be popularly implemented in carbonate reservoirs (Manrique et al., 2010). Chemical and gas EOR methods are however regularly implemented in carbonate reservoirs. An important aspect to EOR in carbonate reservoirs is wettability alteration, as carbonates generally are characterized by oil-wet or mixed-wet conditions.

Two techniques that are especially interesting for EOR in carbonates are smart water injection and CWI, as they have the potential to alter the wettability in carbonates. Carboxylic acids play a significant role in dictating the wettability alteration. Several studies have concluded that carbonates containing lower acidic oils generally exhibits more water wet behavior (S. Jafar Fathi et al., 2010; Standnes & Austad, 2000; Zhang et al., 2007). Lowering the AN of the oil leads to higher affinity towards water, and subsequently increasing oil recovery.

### 2.7.1 Smart water injection

Smart water as an EOR technique involves adjusting the property of the injected water to optimize production. As an EOR technique, smart water injection is considered as an

economically viable and environmentally friendly alternative. The injected water can be modified by adjusting the salinity and ionic composition (S. Jafar Fathi et al., 2010). An important attribute of smart water injection is the ability to alter the wettability of natural carbonate reservoirs towards a more water-wet system.

The surface charges on carbonate reservoirs are an important aspect to the wettability of carbonate reservoirs. Ionic composition of smart water, and its effect on the surface charges has been greatly studied (Rezaei Doust et al., 2009; Zhang et al., 2007). Both studies concluded that the active determining ions in the wettability process were $Ca^{2+}$, $Mg^{2+}$, and $SO_4^{2-}$. Zhang et al. (2007) found that $SO_4^{2-}$ must act together with either $Ca^{2+}$ or $Mg^{2+}$ for improving oil recovery. Temperature must exceed a certain threshold for these ions to alter the wettability of carbonate surfaces, and as temperature increases the effect of the ions increases. Figure 2.9 illustrates suggested mechanisms for wettability alteration through $SO_4^{2-}$ active ions on carbonate surface.

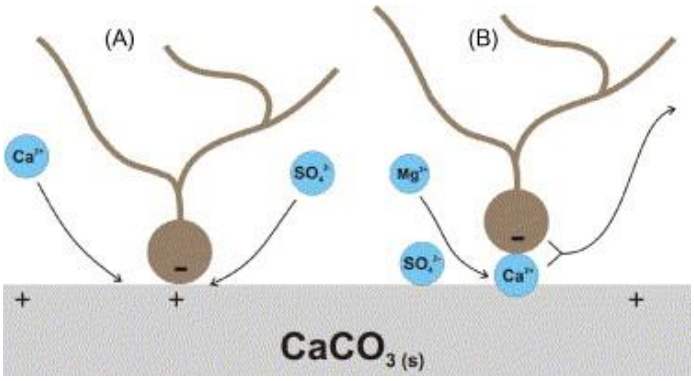


**Figure 2.9** Illustration of suggested mechanism for wettability alteration **(a)** $Ca^{2+}$ and $SO_4^{2-}$ active ions. **(b)** $Mg^{2+}$ and $SO_4^{2-}$ active ions. (Zhang et al., 2007)

### 2.7.2 Carbonated water injection

CW is also a technique used for EOR and is the premise of this thesis. It is not considered a smart water technique as the main object is not to change the ionic composition of the injected water, but rather dissolving the $CO_2$ in the water to form a single phase. Several mechanisms have been suggested when it comes to CWI, mainly viscosity reduction, wettability alteration, and oil swelling. Viscosity reduction and oil swelling is due to $CO_2$ from CW dissolving in the oil phase.

An essential element to CW is the dissolution of $CO_2$ in the water. As $CO_2$ dissolve in the water it experience both increase in density and viscosity, and eliminating some challenges faced in pure $CO_2$ injection (Bisweswar et al., 2020). The amount of $CO_2$ dissolving in the water is dependent mainly on temperature and pressure. Figure 2.10 is a great representation of the behavior of $CO_2$ for different temperatures and pressures. From this we can see that the $CO_2$

has an affinity towards liquid phase at high pressure and temperature. The theory therefore suggests that more $CO_2$ is dissolved in the water phase at high pressure.

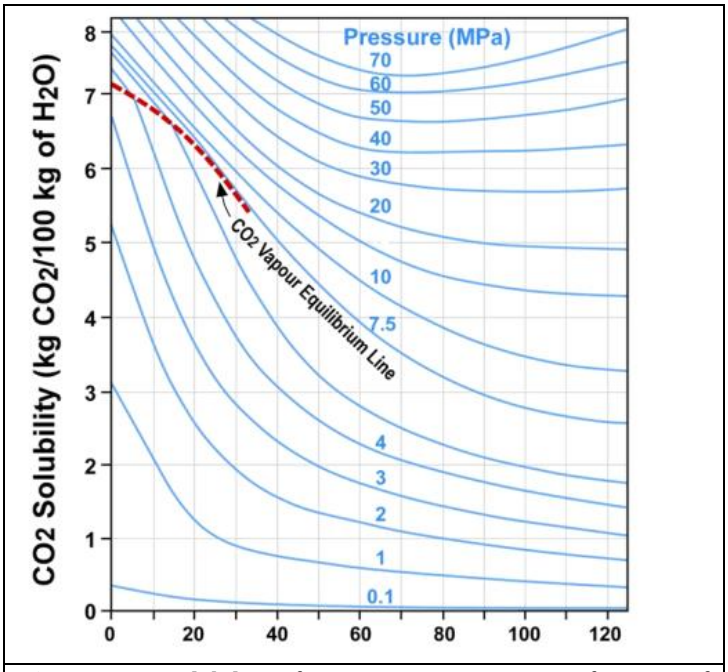


**Figure 2.10** Solubility of $CO_2$ in pure water as a function of temperature [℃] (Perkins & Innovates, 2003)

Injecting the CW at high pressure should therefore increase the effect of mass transfer of $CO_2$ into the oil phase. While $CO_2$ increases the water viscosity, it simultaneously decreases viscosity of the oil phase. This can lead to a better mobility ratio. Figure 2.11 is an illustration of CWI leading to better mobility ratio and reducing the viscous fingering effect from pure $CO_2$. As more $CO_2$ is transferred to the oil phase the more the viscosity reduces and the oil swells, causing liberation of trapped oil.

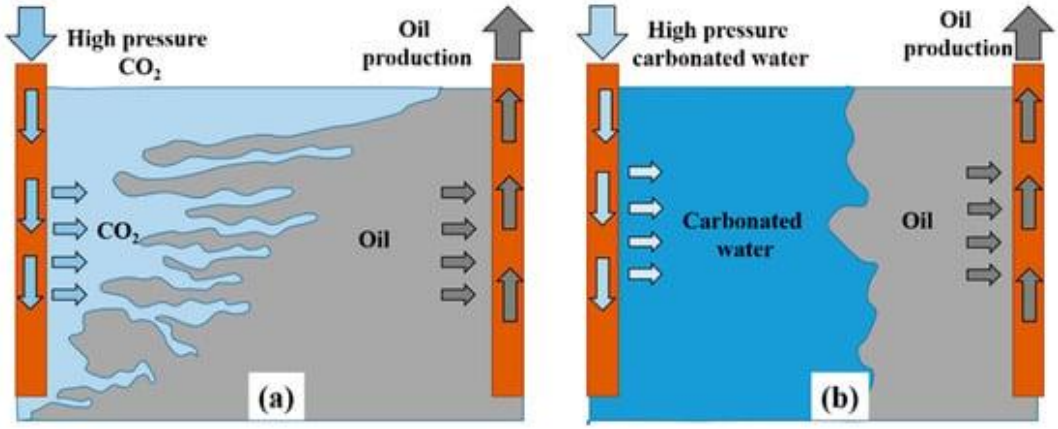


**Figure 2.11** Oil displacement through **(a)** $CO_2$ injection **(b)** CW injection (Hamouda & Bagalkot, 2019)

A mechanism that is extra relevant for carbonate reservoirs is the wettability alteration. Drexler et al. (2020) conducted experiments and confirmed the effect of CW decreasing the pH of the aqueous phase and subsequently altering the wettability. As this increases the positive charge at the interface the system shifts towards a more water wet character.

Newer studies look towards combining smart water and CW to form hybrid smart CW. Soleimani et al. (2021) conducted experiments with carbonated smart water injection in carbonate reservoirs. They concluded that both the $CO_2$ volume and brine composition were important for the oil recovery factor. From these studies it was observed that when the salinity of the brine was increased from 2000 to 40000 ppm, the recovery decreased for the CW.

Ghosh et al. (2022) has also investigated carbonated smart water. Results from their experiments showed that addition of sulfate in the CSW increased the oil recovery. It was also concluded from their study that carbonated smart water reduced the IFT considerably compared to ordinary CSW.

In addition to enhancing the oil recovery, CWI works as carbon sequestration. The industry is continuously looking towards reducing emissions through carbon storage, and CWI is therefore a technique that should be sustainable and relevant in the future. Figure 2.12 is an illustration of the phase diagram of $CO_2$. This is an essential part of carbon storage, as $CO_2$ in liquid phase is easier to deal with. Analyzing optimal liquification pressure is important as the liquification process is costly.

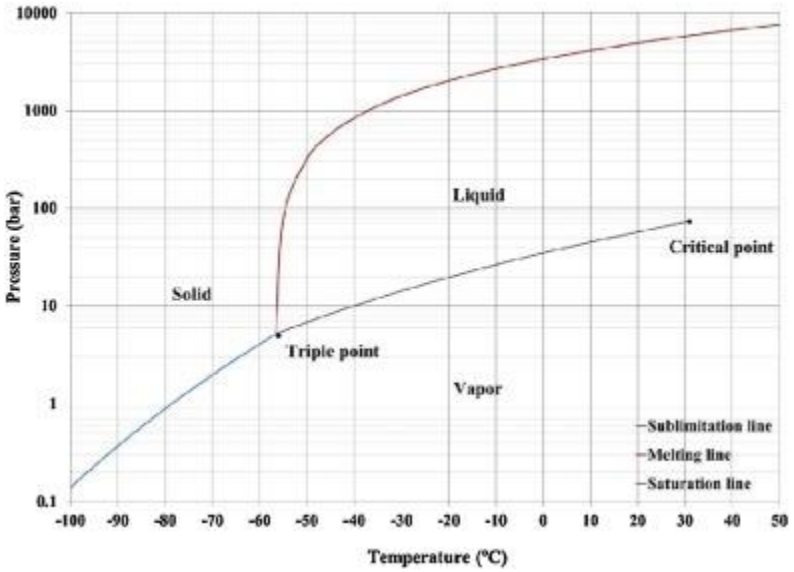


**Figure 2.12** Phase diagram of $CO_2$

# 3. Experimental section

## 3.1 Materials

### 3.1.1 Core material

Stevns Klint chalk was chosen as the core material for this experiment as it holds significant relevance, because it provides a representation of the North Sea chalk reservoir, mainly the Ekofisk field. Located in Denmark, Stevns Klint chalk exhibits similar geological and petrophysical properties to the carbonate formations found in the North Sea. Its composition is characterized by high porosity, usually between 40-50%, and low permeability, usually between 2-5 mD (Frykman, 2001; Puntervold et al., 2007). The Stevns Klint chalk outcrop was drilled into several cores, which then were cut to desired lengths of around 7 cm, and then shaped into desired diameters of around 3.80 cm. Figure 3.1 is a scanning electron microscope (SEM) photo conducted on Stevns Klint chalk.

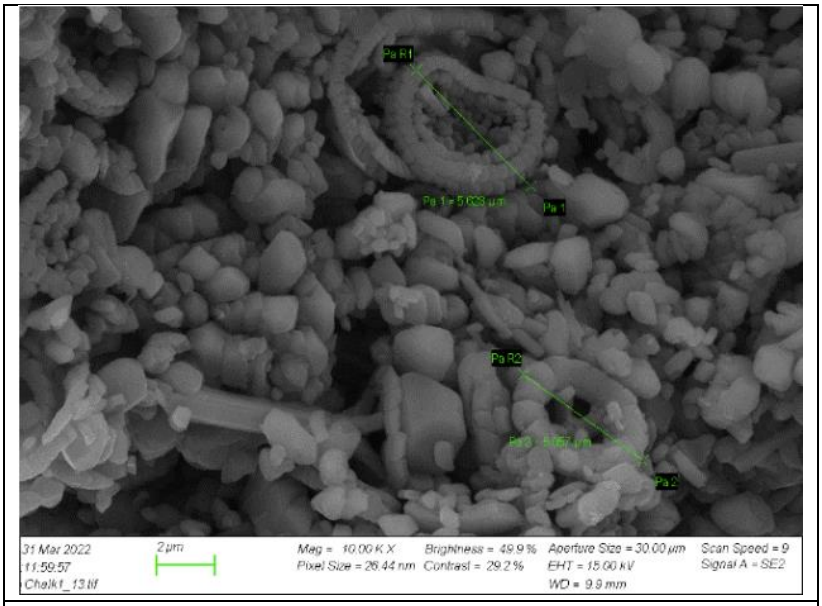


**Figure 3.1** SEM-photo of Stevns Klint chalk (Khan et al., 2023)

The procedure of preparing the core material is illustrated in figure 3.2.


**Figure 3.2** a) Stevns Klint outcrop chalk b) Drilled cores c) Shaping of desired core diameter after cutting

Equation 3.2 for calculating the pore volume is presented in section 3.3.2. Equation 2.1 from section 2.2.1 was then used to calculate the porosity, and equation 2.2 from section 2.2.2 was used to calculate the permeability. Examples of these calculations are all presented in the appendix. Results from the measurements and calculations of the cores physical properties are all summarized in table 3.1.

**Table 3.1** Physical properties of the Stevns Klint cores used for the experiments

| Core nr. | Length (cm) | D (cm) | PV (mL) | Oil volume (mL) | ϕ (%) | k (mD) |
|---|---|---|---|---|---|---|
| **SK1** | 6.89 | 3.80 | 38.42 | 34.49 | 49.2 | 3.2 |
| **SK2** | 6.80 | 3.80 | 37.77 | 33.91 | 49.0 | 2.9 |
| **SK3** | 6.87 | 3.81 | 36.84 | 31.69 | 47.0 | 3.4 |
| **SK4** | 7.14 | 3.79 | 40.09 | 36.12 | 49.8 | 3.2 |
| **SK5** | 6.86 | 3.80 | 36.81 | 33.00 | 47.3 | 3.1 |

### 3.1.2 Oil preparation

The base oil used in this experiment is referred to as Heidrun crude oil, as it comes from the North Sea Heidrun oil field. This was diluted with 40% n-heptane and left for magnetic stirring to reduce the viscosity of the base oil, making it easier for laboratory experiments. After mixing 60% Heidrun oil and 40% n-heptane the oil is then referred to as RES-40. In the next step, RES-40 was heated to 60℃, further decreasing the viscosity, to make the filtering process easier. The oil was then filtered using 5 μm Millipore filter to reduce the possible impurities.

Anton Paar DMA 4500 density meter was used to measure the density of the oil, and Anton Paar MCR 302 rheometer was used to calculate the viscosity. The procedures of these

measurements are presented in the next subchapter. All the results of the measured physical properties are summarized in table 3.2.

**Table 3.2** Physical properties of Heidrun base oil and RES-40 test oil

| **Oil** | **ρ** $[\mathbf{g/cm^3}]$ | **AN [mg of KOH/g]** | **μ [cP] at 20℃** | **μ [cP] at 50℃** |
|---|---|---|---|---|
| Heidrun base oil | 0,893 | 2.82 | 24.4 | - |
| RES-40 | 0.806 | 1.8 | 2.3 | 1.5 |

### 3.1.3 Preparation of brines

The brines were made in the laboratory by adding salts to distilled water. Both the SW and FW, VB0S, were made based on the real values from the North Sea Valhall field. The composition and physical properties of the brines are presented in table 3.3.

**Table 3.3** Composition of ions and physical properties of the brines

| | **SW** | | **VB0S** | |
|---|---|---|---|---|
| **Ions** | m, g/l | M, mole/l | m, g/l | M, mole/l |
| $HCO_3^-$ | 123 | 0.002 | 567 | 0.009 |
| $Cl^-$ | 18617 | 0.525 | 37795 | 1.066 |
| $SO_4^{2-}$ | 2306 | 0.024 | 0 | 0.000 |
| $Mg^{2+}$ | 1082 | 0.045 | 189 | 0.008 |
| $Ca^{2+}$ | 520 | 0.013 | 1160 | 0.029 |
| $Na^+$ | 10347 | 0.450 | 22911 | 0.997 |
| $K^+$ | 393 | 0.010 | 207 | 0.005 |
| **Properties** | | | | |
| Density, [g/ml] | 1.026 | | 1.040 | |
| Weight, [%] | 3.24 | | 6.53 | |
| TDS, [g/l] | 33.39 | 33.39 | 62.83 | 62.83 |
| Ionic strength, [mole/l] | | 0.657 | | 1.112 |
| $Ca^{2+}/SO_4^{2-}$ | | 0.540 | | |

The FW is referred to as VB0S, which is an abbreviation of Vallhall Brine 0 Sulfate, as it does not contain any $SO_4^{2-}$ - ions. It is important to make sure that the carbonate and chlorides are well mixed, so they are initially left for magnetic stirring in separate flasks, after proper mixing the carbonates and chlorides are mixed in a single flask. This is done to reduce the risk of precipitation. A high relative amount of carbonate compared to chlorides may cause precipitation without proper precautions.

The relative amount of carbonate compared to chlorides is low for the SW composition, so carbonate precipitation is not an issue when it comes to SW preparation. However, contrary to FW, SW contains sulfate that can cause precipitation when mixed with chlorides. Two separate flasks are therefore needed for SW preparation as well. The chlorides are mixed separately from the sulfate to reduce the risk of precipitation. After some time, the chlorides and sulfate are mixed in a single flask using magnetic stirring. When the chlorides and the sulfate are properly mixed separately, they are then added to a single flask.

After mixing, the brines were filtrated using a 0.22 μm Millipore filter. This is done to get rid of possible impurities. During this process a pump is connected to the flask for vacuum. Figure 3.3 shows the filtration set-up used in the brine preparation.

**Figure 3.3** Filtration set-up

### 3.1.4 Carbonated FW preparation

The CFW was prepared for two different injection pressures, 50 bars and 10 bars. This process involves the use of a $CO_2$-cylinder, an equilibrium cell filled with de-ionized (DI) water filled in the top chamber, a piston cell with FW filled in the top chamber, and a transfer cell filled with DI water in the top chamber. For illustrations see figure 3.x. The preparations methods

were a bit different for the high injection pressure compared with the low injection pressure. Consequently, the preparation methods will be presented individually.

**High pressure (50 bars)**

The first step of high-pressure carbonated CFW preparation was to inject $CO_2$ into the equilibrium cell at 10 bars, during which 600 ml of DI was bled from the equilibrium cell. Following this there was now 600 ml of $CO_2$ in the equilibrium cell at 10 bars. The bleeding valve was then closed, and FW was then injected from the piston cell into the equilibrium cell until the pressure of 20 bars was reached. The equilibrium cell was now filled with 600 ml of $CO_2$ and FW at 20 bars. Equilibrium cell with $CO_2 + FW$ was then left to equilibrate overnight. The pressure in the equilibrium cell fell to 17 bars overnight due to $CO_2$ dissolving into the FW, so the equilibrium cell was re-pressurized by injecting DI into the cell and leaving the $CO_2 +$ FW side closed. The $CO_2 + FW$ was then transferred from the equilibrium cell to the transfer cell at 45 bars. 300 ml of DI water was bled from the transfer cell during this process, so there was 300 ml of CFW accumulated in the transfer cell at 45 bars. It was then pressurized until 50 bars. Subsequently, 300 ml of high-pressure CFW preparation was finished and ready for use.

**Low pressure (10 bars)**

The method of preparing low-pressure CFW was a little different. In this process, $CO_2$ was injected into the equilibrium cell at 5 bars, during which 300 ml of DI was bled from the equilibrium cell. At this stage there was now 300 ml of $CO_2$ in the equilibrium cell at 5 bars. The bleeding valve was then closed, and FW was then injected from the piston cell into the equilibrium cell until the pressure of 7 bars was reached. The equilibrium cell was now filled with 300 ml of $CO_2$ and FW at 7 bars. Instead of waiting overnight, the $CO_2 + FW$ was transferred from the equilibrium cell to the transfer cell at 7 bars right away. 200 ml of DI water was bled from the transfer cell during this process, so there was now 200 ml of CFW in the transfer cell at 7 bars. DI water was then pumped into the transfer cell at 10 bars with the CFW side left closed. The pressure in the transfer cell is maintained overnight with the help of the pump. This last step is done to avoid pressure drops due to $CO_2$ dissolving in the FW. Subsequently, 200 ml of low-pressure CFW preparation was finished and ready for use.

## 3.2 Measurements

### 3.2.1 Density

The density of the brines and oils was measured using an apparat called Anton Paar DMA 4500 density meter, shown in Figure 3.4. It was cleaned before each test using white spirit and acetone. The apparat was calibrated by first measuring the density of DI water, a reading close to 1.00 g/cm$^3$ would suggest that it was ready for use.

It utilizes oscillating U-tube technology, where the fluid sample is injected. The frequency of oscillation is measured, and since this is directly proportional to the density this will then be automatically calculated by the machine. It can measure a wide variety of fluids, including crude oils, and is known to give reliable results of the density.


**Figure 3.4** Anton Paar DMA 4500 density meter used for density measurement

### 3.2.2 Viscosity

Anton Paar MCR 302 rheometer, shown in figure 3.5, was used to measure the viscosity of the oils. A cup filled with the sample was placed inside the machine. Then temperature and shear rate values were chosen. The machine offers the possibility to change the parameters to evaluate the fluid behavior trends, as it has a heating function. The shear rate does not affect the viscosity of Newtonian fluids, but the temperature does. A shear rate equal to 50 l/s and one measuring point was chosen for this experiment, as only the viscosity value was relevant. The RES-40 oil viscosity was however measured at two different temperatures, T=20 ℃ (room temperature) and T=50 ℃. Logically, the viscosity was measured to be lower at T=50 ℃. The machine started when the temperature was stabilized. It worked by rotating the cup and the torque from the oil sample was measured and converted into shear stress, which was then converted to viscosity.

**Figure 3.5** Anton Paar MCR 302 rheometer used for viscosity measurements

## 3.3 Core preparation

The preparation of cores involves emulating similar properties to the reservoir. The process allows for accurate calculation and measurements of the porosity, permeability, and other characteristics of the cores. After the cores were cut and shaped, they were then cleaned using DI water. The cores were then dried in oven at 90 ℃. When they were completely dry the next step was to establish initial water saturation, and afterwards fill it with oil. After saturating with oil, the core was left for ageing for 14 days before oil recovery test.

### 3.3.1 Core cleaning

The first step in restoration is to properly clean the cores for impurities. Puntervold et al. (2007) concluded that even minor quantities of $SO_4^{2-}$ has a significant influence on the initial wetting condition of the Stevns Klint chalk core. This is therefore a crucial step to get reliable data from the experiment. Distilled water was used for cleaning as it does not swell up chalk, unlike for sandstones. Figure 3.6 shows the cleaning set-up used for this purpose.

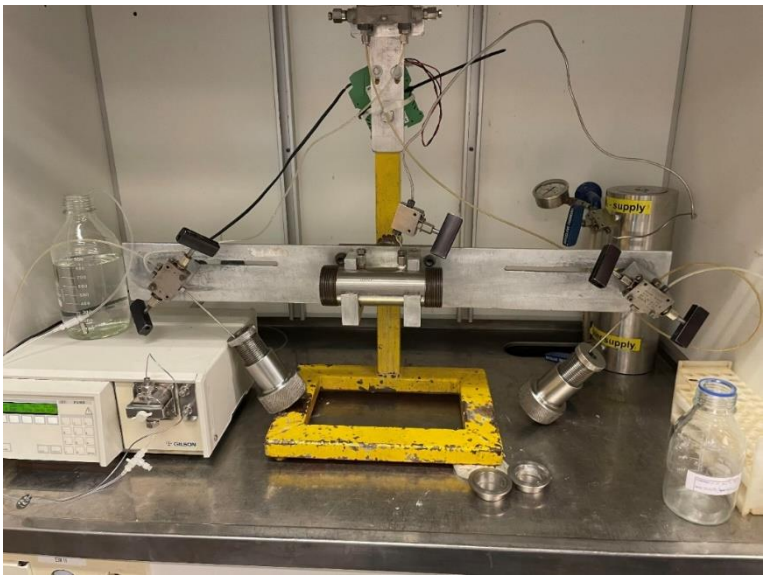

**Figure 3.6** Core cleaning set-up

The cores were cleaned using distilled water. 300 mL of DI water was first pumped through the core at a rate of 0.1 mL/min. The differential pressure was measured when it was stable. Then barium chloride was added to the produced water to check for sulfates. Cloudy appearance suggests there are sulfates still present in the core, and cleaning should then continue. This phenomenon is illustrated in figure 3.7. When there is sulfate still present, the barium from barium chloride will react with sulfate to form barium sulfate, which is the reason for the cloudy appearance. This reaction mechanism is shown in equation 3.1:

$$Ba^{2+}(aq) + SO_4^{2-}(aq) \rightarrow BaSO_4(s) \qquad 3.1$$

The core is clean when the cloudy appearance does not emerge, suggesting that there is no sulfate left.

**Figure 3.7** Example of produced water with $BaSO_4$ precipitation (left) and without $BaSO_4$ precipitation (right)

### 3.3.2 Determining core permeability

After the core is cleaned, the rate is changed to 0.15 mL/min until pressure stabilizes again. Pressure is measured and used for permeability calculations. As flow rate increases the differential pressure should decrease at the same rate, so that the permeability calculation is the same for both rates. A large deviation of the permeability after both rates may suggest that something is wrong with either the pump or the pressure gauge. For this experiment however, no abnormal deviations were observed. As mentioned, the permeability was calculated using equation 2.2.

### 3.3.3 Establishing initial water saturation

After cleaning the cores, they are put in oven at 90℃ for approximately two days, or until the weight stabilizes suggesting that there is no more water left in the core. When the core was completely dry it was then weighed and used for porosity calculation. This was calculated using equation 2.1.

Initial water saturation, $S_{wi}$, was set to 10%. FW was then diluted with 10 times distilled water. The cores were put in a container with marbles underneath to ensure space for saturation at the bottom, and then put in a desiccator. The desiccator containing the container with the core was then vacuumed to ensure that the pores were empty of air. The container was then filled with 10 times diluted FW, and then left for 30 minutes to ensure full saturation. This was done to ensure equal distribution of FW in the pores. An illustration of the set-up used for water saturation is given in figure 3.8. The fully saturated cores were then weighed and used for porosity measurement. The weight was then higher than after core cleaning. As the cores are free from ionic compounds after cleaning, pore volume could then be calculated using equation 3.x:

$$V_P = \frac{m_s - m_{dry}}{\rho_{10*\text{diluted FW}}} \quad 3.2$$

$V_P$ – Pore volume [ml]
$m_s$ – Saturated 10*diluted FW weight [g]
$m_{dry}$ – Dry weight [g]
$\rho_{10*\text{diluted FW}}$ – Density of 10*diluted FW [=1.0026 g/ml]

**Figure 3.8** Set-up used for water saturation

After the core is fully saturated with 10 times diluted FW, the next step is to dry the core until the target weight is reached. This process is a bit delicate since it must slow dry and be closely monitored. It is done by using heated silica placed on the bottom of a desiccator. The cores are then placed on a plate inside the desiccator above the heated silica. Figure 3.9 shows the desiccator used for slow drying. The idea is that the silica gel slowly adsorbs the evaporated water, until the target weight of 10% initial water saturation, $S_{iw} = 10\%$, is reached. Target weight is calculated based on the pore volume calculation:

$$m_{target} = m_{dry} + V_p * S_{iw} * \rho_{10*diluted\ FW} \quad 3.3$$

$m_{target}$ – Target weight [g]
$m_{dry}$ – Dry weight [g]
$\rho_{10*\text{diluted FW}}$ – Density of diluted FW [=1.0026 g/ml]
$S_{iw}$ – Initial water saturation [≈0.1 or 10%]

**Figure 3.9** Desiccator used for slow drying the cores until target weight was reached

After target weight was reached the core was then placed in a sealed container and placed in a cabinet for at least 48 hours to ensure that the FW is evenly distributed through the pores.

### 3.3.4 Oil saturation

After establishing initial water saturation, the core was then placed in a Hassler core holder with a confining pressure at 15 bars to saturate the rest of the pores with RES-40 oil. The system was heated at 50 ℃ to reduce oil viscosity and make the saturation process easier. Both the inlet and outlet line were vacuumed to make sure that there was only oil being pumped in the core, and to remove any air from the core itself. The vacuum process was done after approximately 10 minutes, and the next step was to inject the oil.

Firstly, oil was injected from both the inlet and outlet sides at a rate of 0.5 ml/min until pressure build-up, suggesting that 1 PV has been injected. In the next step, one outlet and inlet side are closed to inject oil through the core, to adsorb acids and bases. In this step 2 PV is injected at a rate of 0.2 ml/min. After 2 PV was injected, we switched the injection side and repeated the process. So, in total 5 PV of RES-40 oil is injected in this process. The heat was then turned off, so that the system could cool down. After the system two hours the core was then pressurized again, as in the first step. This is to make sure that the oil is evenly distributed throughout the core. Normally in this case, only a few ml will be injected before we get pressure-buildup, as the core already should be filled with oil. The produced oil was then used for the next process, ageing.

### 3.3.5 Ageing

The core was then taken out from the holder to prepare for ageing. In this process the core is wrapped with Teflon tape, which works as an excellent seal. This is employed to prevent the

adsorption of excessive, unrepresentative active polar organic components on the outer surface, as this may impact the oil recovery test (Standnes & Austad, 2000). After the core is wrapped it is then placed in an ageing cell with marbles underneath, to increase the contact surface area. The ageing cell is then filled with the produced RES-40 oil, and then closed. It is then put in an oven for 14 days, at 70 ℃. After this the ageing cell is put outside the oven for a day to cool down. The Teflon tape is then unwrapped, and the final weight of the core is measured before the oil recovery test. Original oil in place, OOIP, can now be calculated:

$$OOIP = \frac{\left(m_t - m_{dry} - m_{S_{iw}}\right)}{\rho_{oil}} \quad 3.4$$

$m_t$ – Total weight after ageing [g]
$\rho_{oil}$ – Density of oil [=0.806 g/ml]

Assuming full saturation of oil, then the initial oil saturation, $S_{oi}$, should be expressed as:

$$S_{oi} = 1 - S_{iw} \approx 0.9 \quad 3.5$$

Figure 3.10 showcases the different steps involved in the ageing process.

(a) (b) (c)

**Figure 3.10 (a)** Core wrapped in Teflon tape before ageing **(b)** Core placed in ageing cell **(c)** Unwrapped core ready for oil recovery test

## 3.4 Oil recovery test

After ageing the cores were then ready for oil recovery tests. Both SI and FI were performed during the experiments.

### 3.4.1 Spontaneous imbibition using FW

Two of the cores were put through SI before viscous flooding (VF). These were placed in a cell similar to the one in figure 3.x (b), with marbles underneath the core to increase the contact surface area. The cells were then filled with brine, being FW, VB0S, in this case. They were then put in an oven at 70 ℃. A piston cylinder located outside the oven was then filled with brine at the top, with nitrogen providing pressure equal to 10 bars at the bottom. This cylinder was connected to the cell in the oven to provide it with constant influx of FW. The cell was also connected to a burette located outside the oven on the other side. Continuous measurements were done by opening the valve until it only produced water. Both cores performed the test simultaneously and was concluded after 20 days.

After SI the cores went through FI. SI of FW was performed as it indicates the initial wettability of the cores. If the results are similar between two cores it means that the initial wettability is similar after the core preparation process and that the results from FI received after SI are comparable. By doing this it is possible to analyze the effect of AN and wettability.

Figure 3.11 shows the experimental set-up used for SI.

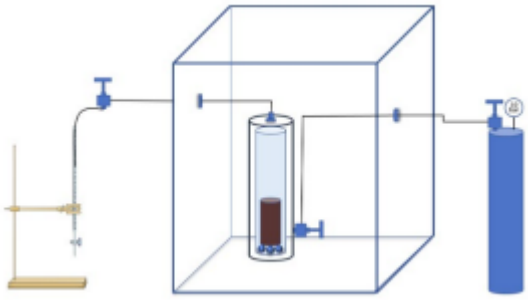

**Figure 3.11** Illustration of the SI set-up (Khan et al., 2023)

### 3.4.2 Forced imbibition/viscous flooding using FW, SW, and CFW

The main experiment involved FI with different injection strategies. Three of the five cores were placed for VF right after ageing, while the two others went through SI beforehand as explained in the last subchapter. The oil recovery test by FI was done both at high and low injection pressure, using different set-ups.

Both set-ups used an oven that was heated at 70℃. Before the tests started all the valves except for the CFW-cylinder were left open, this was done to fill the lines with FW and displace the air. The bypass valve was closed when the desired, constant pressure in the system was reached.

Injection fluid would now only be injected from the inlet, and through the outlet. It was now displacing and producing oil from the core, into the sample burette. As the outlet line was filled with FW before starting the test this had to be measured as "dead volume" when the first oil droplet was produced. The dead volume is subtracted from the pore volume injected, to get accurate readings.

The set-up used for high injection pressure was made from scratch before starting the first test. All the metal lines were cut after careful measurements, to fit the cylinders and core holder positions. The first test was done at a high injection pressure of 50 bar, with a confining pressure of 70 bars. Injection pressure was maintained by having two back pressure valves, one at 50 bars, and another one at 20 bars as a back-up. In this set-up, the injection fluids were placed inside the oven together with the core holder so that it was already heated before passing through the core. The core was wrapped in aluminum tape before being placed inside the core holder (see figure 3.12). This was done to ensure that the injection fluid was going through the core instead of alongside it, as this was performed at high injection pressure. $CO_2$ can swell the rubber sleeve, meanwhile the aluminum wrapping is not affected by $CO_2$. Only one injection strategy was tested using this set-up, as some problems occurred which will be discussed in the next chapter. FW was injected in secondary mode, and CFW was injected in tertiary mode.

**Figure 3.12** Core SK 1 wrapped in aluminum tape before high pressure FI oil recovery test

Figure 3.13 shows the different components involved in the high-pressure set-up. The blue outline represents the oven, so the injection fluid is heated.

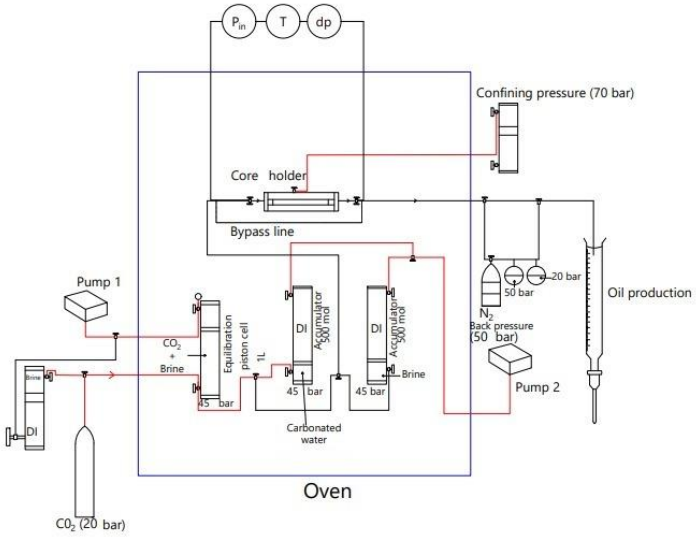


**Figure 3.13** Illustration of high-pressure FI set-up

The injection pressure of the second set-up was at 10 bars, with a confining pressure of 15 bars. Injection pressure was maintained by having a back-pressure valve at 10 bars. In this set-up the injection fluids were placed outside the oven at room temperature, contrary to the high-pressure set-up. Four tests were performed, and several injection strategies were employed in this set-up. The strategies involved CFW injection in secondary and tertiary mode. Only two of the cores went through FI, while the last two cores went through SI prior to FI.

Figure 3.14 shows the different components involved in the low-pressure set-up. Here the injection fluids are located outside the oven.

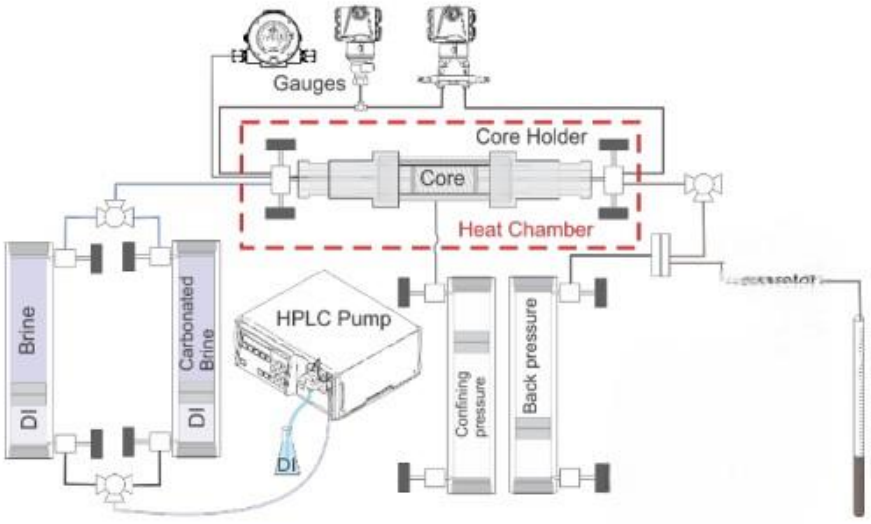


**Figure 3.14** Illustration of low-pressure FI set-up. Modified from (Khan et al., 2023)

Table 3.4 shows all the injection strategies. There were variations on the duration periods of each test.

**Table 3.4** Injection strategies involving SI and FI

| Core nr | Fluid pressure | SI (20 days) | FI-Step 1 (1 PV/day) | FI-Step 2 (1 PV/day) |
|---|---|---|---|---|
| **SK 1** | 50 bars | - | FW | CFW |
| **SK 2** | 10 bars | - | FW | CFW |
| **SK 3** | 10 bars | - | CFW | SW |
| **SK 4** | 10 bars | FW | CFW | FW |
| **SK 5** | 10 bars | FW | FW | CFW |

# 4. Results and discussion

Results from the experiment with FI at high injection pressure and low injection pressure, as well as SI at low pressure will be presented in this chapter. The FI experiments were all done at injection rates of 1 pore volume a day, with five different injection strategies. All the tests were done at 70℃.

## 4.1 Oil recovery at high injection pressure

The first test was done at a high injection pressure of 50 bars.

### 4.1.1 Forced imbibition with formation water and carbonated formation water in tertiary mode

For the first FI test FW was injected at high pressure followed by CFW injection. Figure 4.1 is a representation of the recovery percentage of original oil in place, %OOIP, as a function of the pore volume injected, for SK1. In total, 5.0 PV of FW and CFW was injected during this test and the recovery was 72.1 %OOIP.

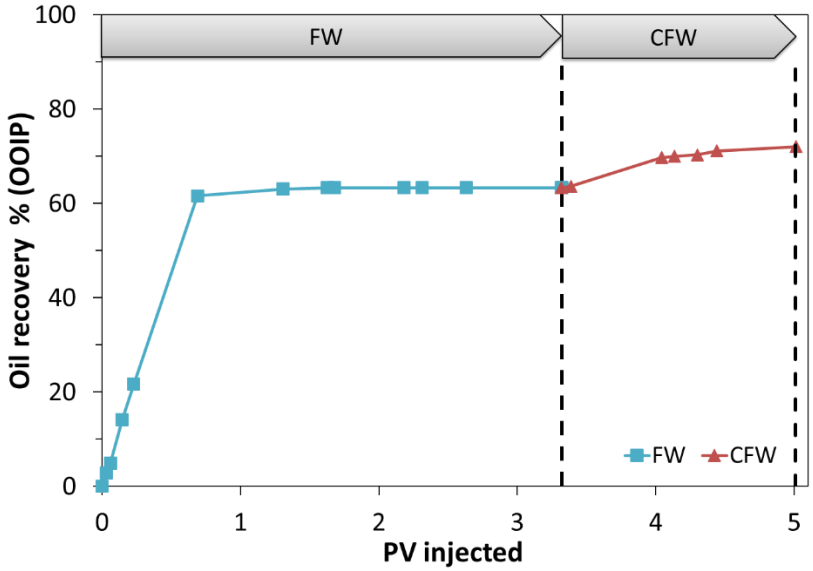


**Figure 4.1** Oil recovery through FI of SK1 with FW-injection in secondary mode and CFW-injection in tertiary mode at high pressure. Test conducted at T=70℃ and P=50 bars.

There were some technical problems occurring during this test. In the same evening the test started, the power in the lab went off, and consequently the pump stopped. This was noticed when arriving at the lab the morning after. However, the pore volume injected was adjusted after the technical problems, as the total production was recorded, making it possible to calculate how long the pump was off.

The exact point of water breakthrough, WBT, was not recorded, due to the technical problems mentioned. Nevertheless, the first point after WBT was recorded at 0.7 PV injected. Only 1.7 %OOIP recovery was produced from this point until plateau was reached. FW injection plateau was reached after 1.6 PV injected; no oil was produced through FW beyond this point. The %OOIP produced from FW was 63.4%. After 3.3 PV of injected FW, represented by the first dashed line, the system was switched to CFW injection.

The pump stopped again between 0.8 and 1.1 PV of injected CFW, this time due to pressure build-up in the system. 6.9 %OOIP was produced from injected CFW up until this point. From the measurement of total production, I could calculate that the pump had been off for 1 hour before it was noticed, and PV injected could be adjusted again. The injection pressure had now exceeded the high-pressure limit of 60 bars, even though the injection pressure was supposed to be at only 50 bars. Obviously, there were some problems in the system, but the high-pressure limit was increased to 66 bars to try and see if was possible to get some more production. Remember, the confining pressure of the core was at 70 bars, so the pressure limit had to be under that. There was 1.7 %OOIP production after the first pressure build-up before the pump stopped again, as it exceeded the new high-pressure limit of 66 bars. It was then decided to finally stop the test, even though the production during CFW injection was yet to reach the plateau. The test ended with 1.7 PV of CFW injected and recovery of 8.7 %OOIP, illustrated by the second dashed line.

From figure 4.2 it looks like the confining pressure of 70 bars exceeded the yield pressure point of the core material, as the core disintegrated and changed into a paste-like form after the test. It was also discovered that the back pressure valve was blocked during the test, most likely due to a failed membrane. Both these findings help explain why there was a pressure build-up during CFW injection.

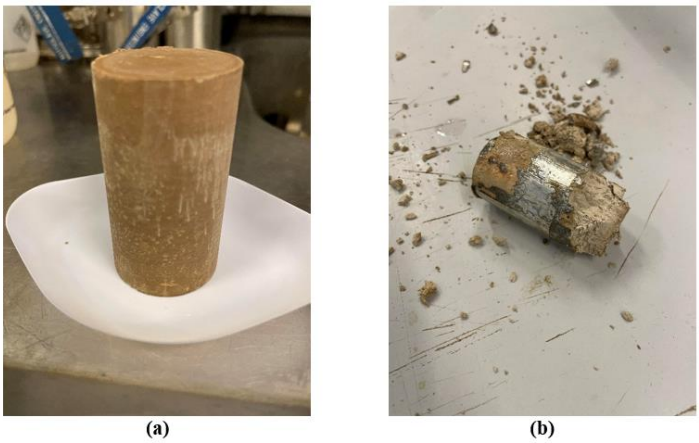


**Figure 4.2** Illustration of SK1 (a) Before FI (b) After high pressure FI

## 4.2 Oil recovery at low injection pressure

It was then decided to switch to a low-pressure FI set-up for the next tests, as there were some occurring challenges with the high-pressure set-up. All the tests in this subchapter were performed at low injection pressure of 10 bars.

### 4.2.1 Forced imbibition with formation water and carbonated formation water in tertiary mode

For the second FI test FW was injected at low pressure followed by CFW injection. Figure 4.3 is a representation of the recovery percentage of original oil in place, %OOIP, and pressure drop as a function of the pore volume injected, for SK2. In total, 7.2 PV of FW and CFW was injected during this test and the recovery was 75.2 %OOIP.

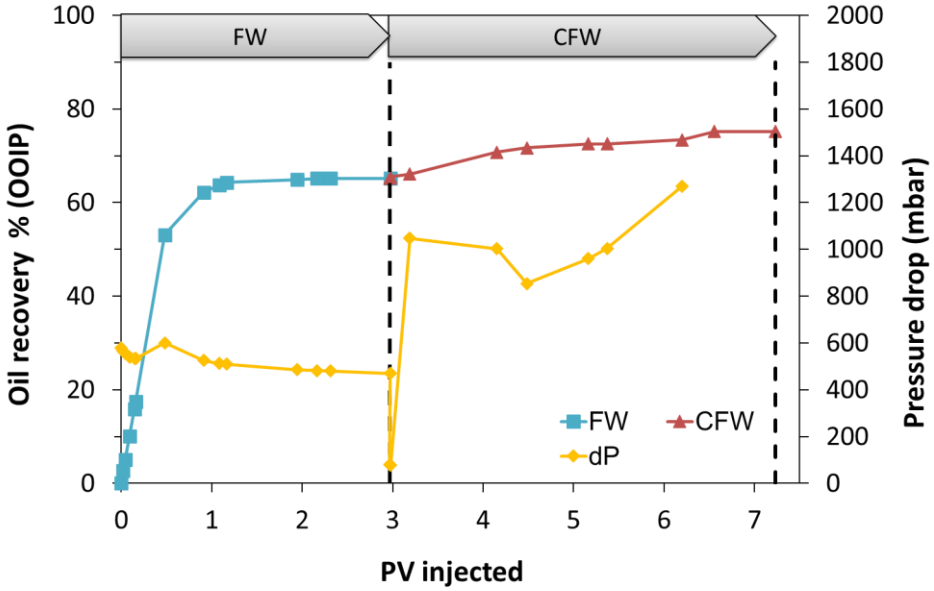


**Figure 4.3** Oil recovery and pressure drop through FI of SK2 with FW-injection in secondary mode and CFW-injection in tertiary mode. Test conducted at T=70℃ and P=10 bars.

The WBT was measured at 0.48 PV of FW injected and recovery of 53.1 %OOIP. Plateau was reached at 2.2 PV of FW injected and 65.2 %OOIP recovery. The system was then switched to CFW injection when 2.97 PV of FW had been injected. An additional production of 10.03 %OOIP was obtained during CFW injection. The plateau was reached after 3.6 PV of CFW injected, and the test was stopped after 4.3 PV of CFW injected.

The pressure drop was measured at every point. It decreased slightly in the beginning of the test, before increasing again up until the WBT point. After the WBT point the pressure drop slowly decreased until an almost constant value. The pressure drop increased significantly when the system switched to CFW injection, from around 500 mbar to around 1000 mbar. There was an increase in pressure drop until the test was stopped.

### 4.2.2 Forced imbibition with formation water and carbonated formation water in secondary mode

For the third FI test CFW was injected at low pressure followed by FW injection. Figure 4.4 is a representation of the recovery percentage of original oil in place, %OOIP, and pressure drop

as a function of the pore volume injected, for SK3. In total, 3.8 PV of CFW and SW was injected during this test and the recovery was 75.7 %OOIP.

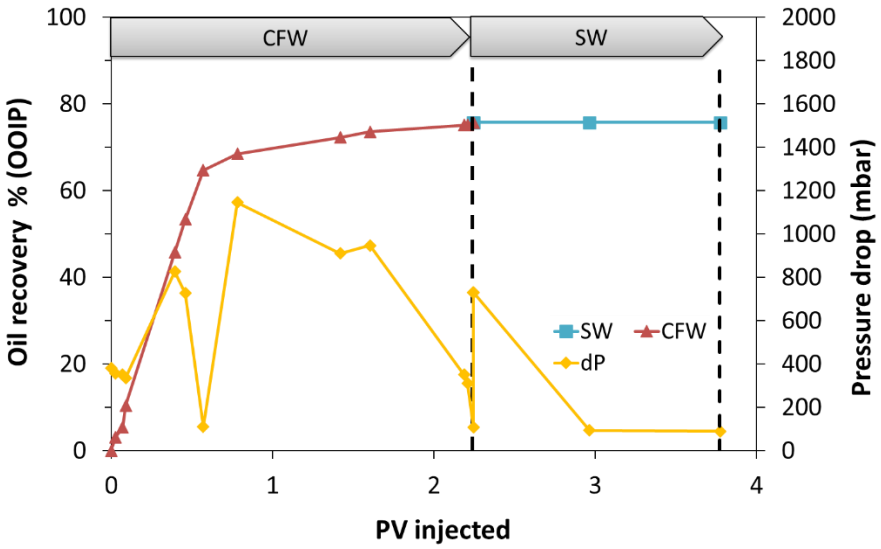


**Figure 4.4** Oil recovery and pressure drop through FI of SK3 with CFW-injection in secondary mode and SW-injection in tertiary mode. Test conducted at T=70℃ and P=10 bars.

The WBT point was measured around 0.6 PV of CFW injected, and a recovery of 64.7 %OOIP. Naturally, as CFW was injected in secondary mode in this test the WBT was measured at a higher recovery than for FW injection in secondary mode. After the WBT point an additional 11.04 %OOIP was produced. Plateau was reached after a total production of 75.7 %OOIP and 2.24 PV of CFW injected.

It was then decided to switch to SW injection, even though there was not expected to be any additional production with SW injection at tertiary mode after CFW injection. CW injection is considered an EOR technique, while SW lacks the chemical properties that make CW effective for EOR in carbonate reservoirs. 1.5 PV of SW was injected before the test was stopped. As expected, there was no additional oil production after CFW injection.

As for the pressure drop curve compared to FW injection in secondary mode from SK2, the difference in trend was only the magnitude of dP change. At the start of the SK3-test the dP had a slight decrease, before accelerating at a high rate until the WBT point. Right after the WBT point the dP had an equally high decelerating rate. The pressure drop curve for CFW injection then experienced extreme fluctuation, so it was difficult to get reliable readings. After switching to SW injection, the dP curve slowly decelerated down to 100 mbar and stabilized.

### 4.2.3 Spontaneous imbibition with formation water

For the last two cores it was decided to do SI before FI test. This was done to check the effect of AN and wettability on oil recovery during CFW injection. Figure 4.5 illustrates the results from the SI test conducted on SK4. The result from recovery percentage of original oil in place, %OOIP, as a function of time (days) is presented.

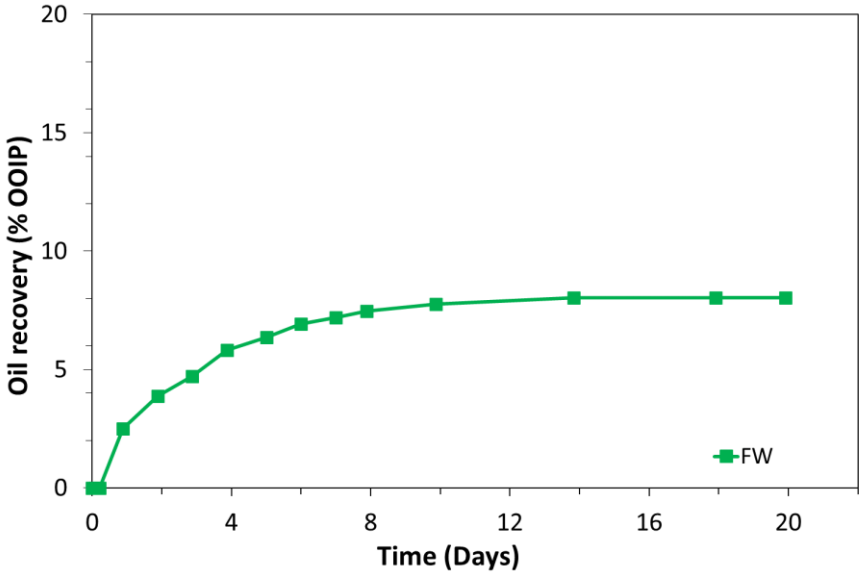


**Figure 4.5** Oil recovery through SI of SK4 with FW. Test conducted at T=70℃ and P=10 bars.

Figure 4.6 illustrates the results from the SI test conducted on SK5. The result from recovery percentage of original oil in place, %OOIP, as a function of time (days) is presented.

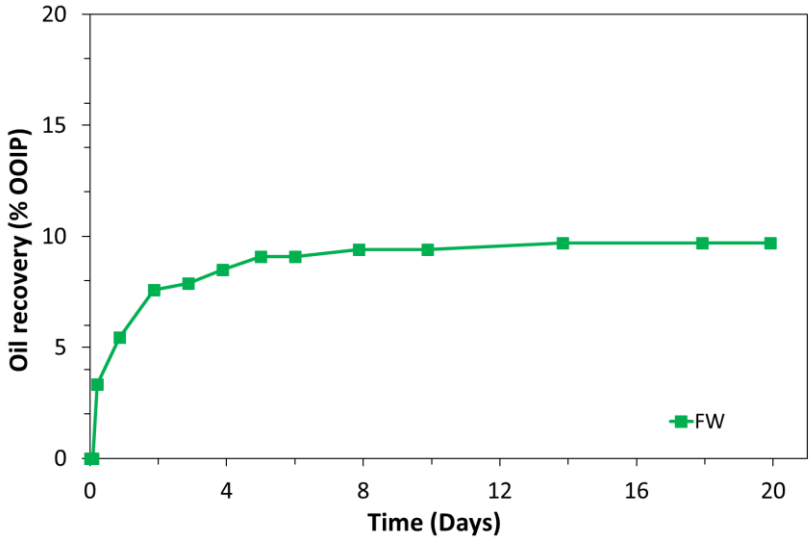


**Figure 4.6** Oil recovery of SK5 through SI with FW. Test conducted at T=70℃ and P=10 bars.

The SI-tests of SK4 and SK5 were done simultaneously. As visualized in figure 4.5 and 4.6 the SI-tests lasted for 20 days before going through FI test. Daily measurements were conducted in the first week, as the recovery rate was quite high then. The recovery rate after a week was less than 0.1 ml/day so less frequent measurements were done from that point. After about 14 days, both cores reached their plateau, and no more oil recovery was measured in the last 6 days. Total recovery for SK4 and SK5 were 8.0 and 9.7 OOIP% respectively.

In this study, the two cores were prepared in the same manner, and yielding similar results. Both cores exhibited a slightly water-wet nature, indicating that the preparation process of the cores was dependable and consistent. The similarity in the results suggests that a fair comparison can be made between the cores. This allows for a more comprehensive understanding of the fluid-rock interaction.

### 4.2.4 Forced imbibition after spontaneous imbibition with formation water and carbonated formation water in secondary mode

After SI, SK4 was put through FI with CWF injection in secondary mode. Figure 4.7 is a representation of the recovery percentage of original oil in place, %OOIP, and pressure drop as a function of the pore volume injected, for SK4. In total, 3.0 PV of CFW was injected during this test and the recovery was 72.8 %OOIP.

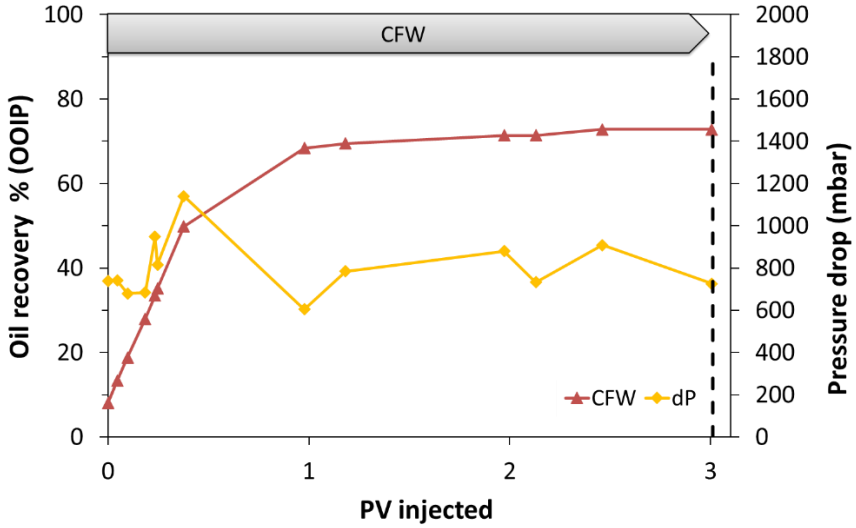


**Figure 4.7** Oil recovery and pressure drop after SI through FI of SK4 with CFW-injection in secondary mode. Test conducted at T=70℃ and P=10 bars.

The exact WBT point happened late in the evening and was not measured, but the last point before WBT was measured around 0.38 PV of CFW injected, and a recovery of 49.8 %OOIP.

After this an additional 23.0 OOIP% was produced. Plateau was reached after a total production of 72.8 %OOIP and 2.5 PV of CFW injected. An additional 0.6 PV was injected before deciding to end the test.

As for the other tests the pressure drop reached a peak during the WBT point before rapidly decelerating. The pressure drop trend is similar to SK3, which also used CFW injection in secondary mode. After WBT point the dP then experienced some fluctuation but stabilized around 600-900 mbar for the rest of the test.

### 4.2.5 Forced imbibition after spontaneous imbibition with formation water and carbonated formation water in tertiary mode

After SI, SK5 was also put through FI, but this time with FW injection in secondary mode and CWF injection in tertiary mode. Figure 4.8 is a representation of the recovery percentage of original oil in place, %OOIP, and pressure drop as a function of the pore volume injected, for SK5. In total, 5.5 PV of FW and CFW was injected during this test and the recovery was 74.9 %OOIP.

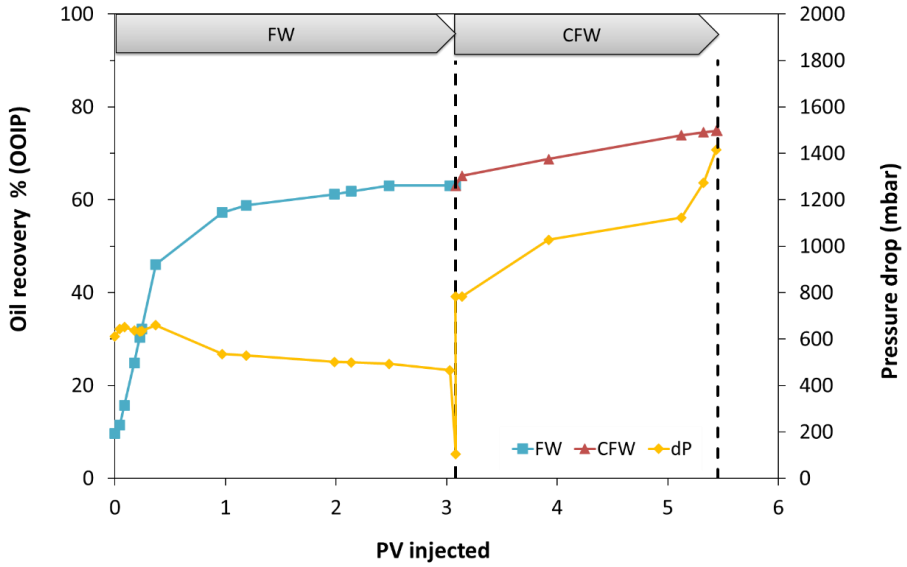


**Figure 4.8** Oil recovery and pressure drop after SI through FI of SK5 with FW-injection in secondary mode and CFW-injection in tertiary mode. Test conducted at T=70℃ and P=10 bars.

The WBT point was measured around 0.4 PV of FW injected, and a recovery of 46.1 %OOIP. After the WBT point an additional 28.8 %OOIP was produced. Plateau was reached after a total production of 63.0 %OOIP and 2.5 PV of FW injected. An additional 0.6 PV was injected before switching to CFW injection. 11.8 %OOIP of additional oil was recovered during CFW injection. The final plateau was reached after 2.4 PV of CFW, and the test was then ended.

The pressure drop curve followed an almost identical trend to SK2. A small dP peak was recorded at the WBT point, before slowly falling. The dP increased rapidly after changing to CFW injection, and then continued to increase until the test was stopped.

## 4.3 Comparison of different injection strategies

All the results from SI and FI tests are summarized in table 4.1.

**Table 4.1** Summary of the results from all the injection strategies

| Core | Injection pressure [bars] | Injection strategy (OOIP% recovery) | | | WBT [OOIP%] | Total recovery [OOIP%] |
|---|---|---|---|---|---|---|
| | | SI | Secondary mode FI | Tertiary mode FI | | |
| **SK1** | 50 | - | FW (63.4) | CFW (8.7) | 61.6 | 72.1 |
| **SK2** | 10 | - | FW (65.2) | CFW (10.0) | 53.1 | 75.2 |
| **SK3** | 10 | - | CFW (75.7) | SW (0.0) | 64.7 | 75.7 |
| **SK4** | 10 | FW (8.0) | CFW (64.8) | - | 49.8 | 72.8 |
| **SK5** | 10 | FW (9.7) | FW (53.3) | CFW (11.8) | 46.1 | 74.9 |

### 4.3.1 Temperature and acid number effect on wettability and oil recovery

The SI test conducted on SK5 is compared to an SI experiment, while the FI test conducted on SK2 is compared to another FI experiment. In both cases, the results obtained from the SI and FI tests are compared to the experiments conducted by (Khan et al., 2023).

In figure 4.9, the two SI experiments were compared to investigate the impact of temperature and AN on wettability and oil recovery in Stevns Klint chalk cores. Test (a) involved oil with AN of 0.58 at a temperature of 110℃, while test (b) conducted on SK5 used oil with AN of 1.80 at a temperature of 70℃. Both tests utilized the same SI setup and core material, with similar length and diameter.

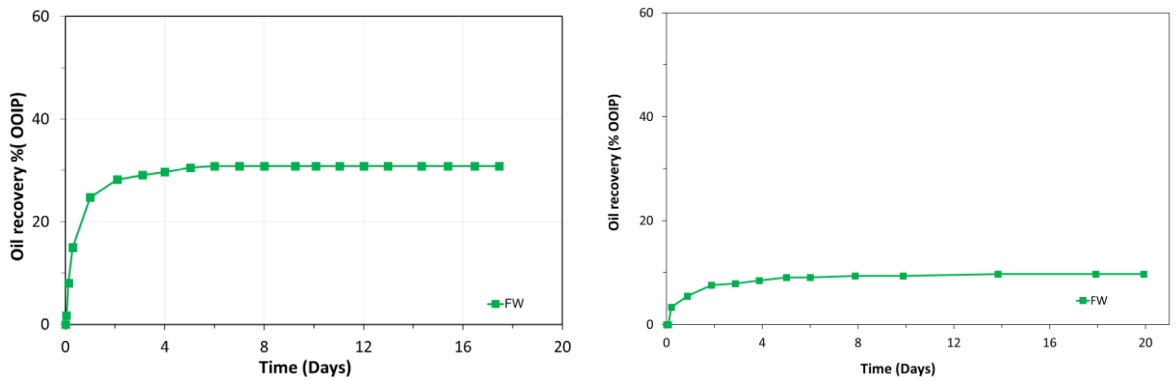


**(a)** **(b)**

**Figure 4.9 (a)** SI into oil (AN=0.58 mg of KOH/g) at 110℃ and P=10 bars (Khan et al., 2023) **(b)** SI into oil (AN=1.80 mg of KOH/g) at 70℃ and P= 10 bars (SK5)

The results demonstrate a difference in wettability between the two conducted experiments. Test (a) reached a plateau with a recovery of 31 OOIP%, whereas test (b) achieved a plateau with a recovery of 9.7 OOIP%. The lower acidic oil in test (a) lead to a more water-wet behavior, as indicated by the significantly higher recovery compared to test (b). This suggests that the oil with a higher acidic oil altered the wettability to a weaker water-wet system.

The finding is consistent with several studies (Seyed Jafar Fathi et al., 2010; Standnes & Austad, 2000; Zhang et al., 2007), which also investigated the AN effect on SK-chalk, using a similar SI setup. Their results showed that oils with lower AN had preferential stronger water-wet characteristics and higher recoveries compared to oils with higher AN. The correlation between these findings reinforces the importance of AN in determining wettability and subsequent oil recovery. Figure 4.10 represent SI experiment conducted with different acidic oils.

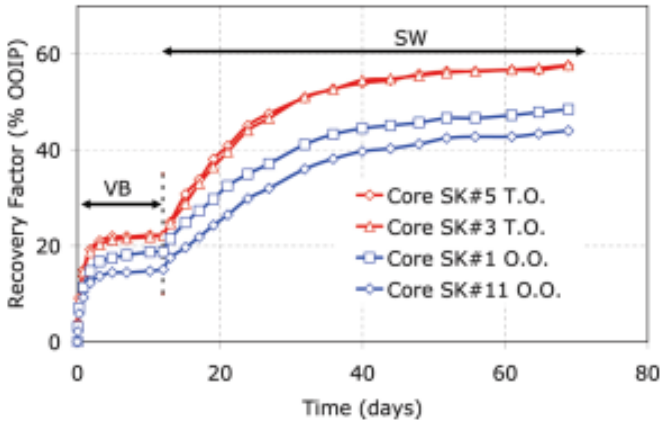


**Figure 4.10** SI experiment conducted by Fathi et al. (2010) at T=110℃ illustrating recovery factor of **(a)** Oil T.O (AN=1.5 mg of KOH/g) and **(b)** Oil O.O (AN=1.8 mg of KOH/g)

Another crucial factor influencing the disparity in oil recovery is the substantial temperature variations between the experiments. Temperature exerts a considerable influence on oil recovery due to its impact on various physical properties. Higher temperatures result in decreased oil viscosity and IFT between the oil and the imbibing fluid, in this case, FW. These effects collectively enhance the oil's ability to flow more easily within the porous media, thereby promoting a higher recovery. Consequently, the temperature differential between the tests plays a pivotal role in facilitating improved oil mobility and overall recovery process for the test conducted at T=110℃.

Building upon the comparison of the temperature and AN effect on SI, the results from the FI tests are then compared with Khan et al. (2023) to further investigate the effect regarding these parameters on the oil recovery. Figure 4.11 illustrates the results of (b) FI in SK2 at

70℃ (AN =1.80), and (a) FI at 130℃ (AN=0.58) conducted by Khan et al. (2023). The total recovery of test (b) was measured at 75.2 %OOIP, after a total of 7.2 PV injected. The total recovery of test (a) was measured at 74.0 %OOIP, after a total of 8.0 PV injected. So, the injection at 70℃ with the higher acidic oil had a 1.3 higher %OOIP recovery, compared to the test conducted at 130℃ with the lower acidic oil. It is important to note that this is not a significant difference as this can also be observed for two identical experiments.

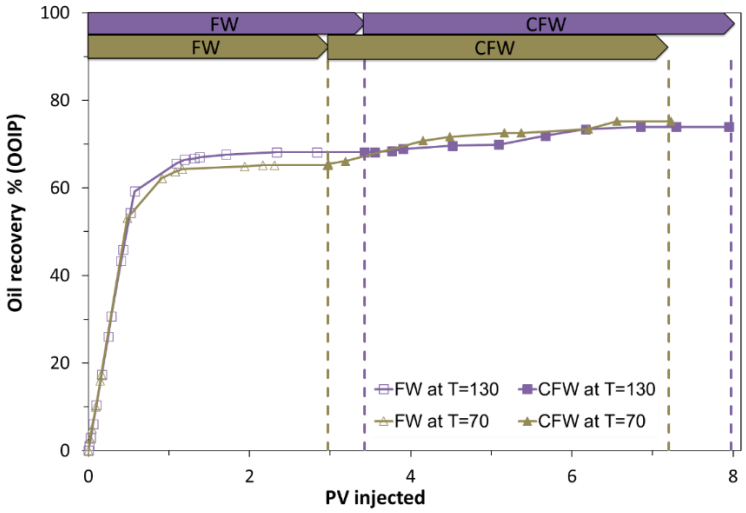


**Figure 4.11** Temperature and AN effect on oil recovery at P=10 bars. Comparison of **(a)** FI in oil (AN=0.58 mgKOH/g) at T=130℃ (Khan et al., 2023) **(b)** FI in oil (AN=1.80 mgKOH/g) at T=70℃ (SK2)

From test (a), the WBT was measured at 0.6 PV of FW injected and recovery of 59.2 %OOIP. Plateau was reached at 2.3 PV of FW injected and 68.2 %OOIP recovery. CFW injection started after 3.4 PV of FW had been injected. The next plateau was then measured after 3.4 PV of CFW injection, and an additional 5.8 %OOIP was recovered from CFW injection. The test was then stopped after injecting 1.1 PV of CFW after the plateau and total recovery of 74.0 %OOIP.

From test (b), the WBT was measured at 0.48 PV of FW injected and recovery of 53.08 OOIP%. Plateau was reached at 2.17 PV of FW injected and 65.17 OOIP% recovery. An additional production of 10.03 OOIP% was obtained during CFW injection, for a total recovery of 75.2 %OOIP.

From the figure 4.9 it was already concluded that the system with the lower acidic oil was more water-wet compared to the higher acidic oil, so it does not look like the wettability influenced the total recovery in FI test. However, test (a) had a higher recovery from the FW injection but ended up with a lower total recovery. In fact, the recovery for the weaker water-wet system, test (a), had a 4.3 OOIP% higher recovery during CFW injection. That is not an insignificant difference.

The AN is higher in SK2 compared to the other test, and subsequently weaker water-wet system. This suggests that the CFW altered the wettability by lowering the AN of SK2.

Wettability alteration is a mechanism involved also for the lower acidic oil, but it is less prominent as the system is more water wet. This would explain the higher recovery during CFW injection of SK2. To summarize, the CFW injection had a larger effect on the recovery of the less water-wet system, as it had more oil trapped in the pores, compared to the stronger water-wet system.

Another factor mentioned earlier is the substantial temperature difference between the two experiments. However, by analyzing and comparing the results of the FI tests this does not seem to influence the recovery process in this case.

### 4.3.2 Pressure effect on oil recovery

The effect of pressure will be discussed in this subchapter. Both high-pressure injection and low-pressure injection were conducted. Figure 4.12 illustrates the results of (a) FI in SK1 at P=50 bars and (b) FI in SK2 at P=10 bars. The total recovery of test (a) was measured at 72,1 %OOIP, after a total of 5.0 PV injected, whereas the total recovery of test (b) was measured at 75.2 OOIP%, after a total of 7.2 PV injected. So, the low-pressure set up recovered 3.2 %OOIP more compared to the high-pressure set up. As mentioned in section 4.1.1, the plateau for the high-pressure set up was not reached due to pressure build up in the system, so the difference in total recovery can be contributed to that.

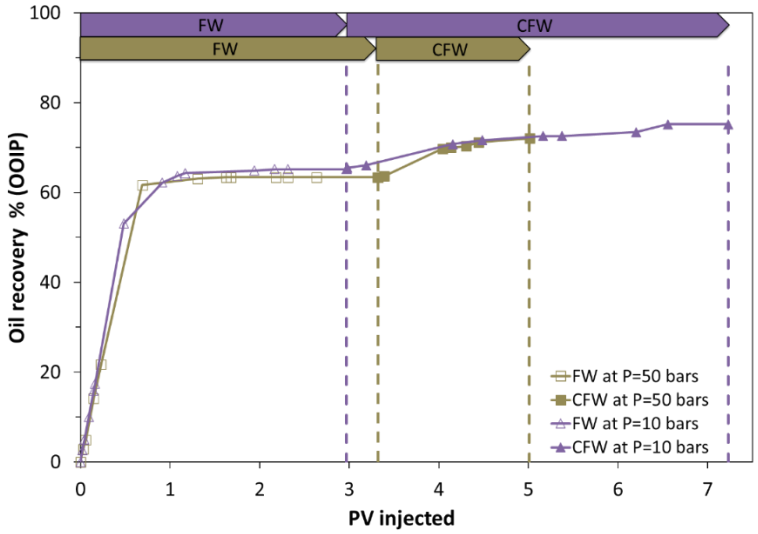


**Figure 4.12** Pressure effect on oil recovery at T=70 ℃. Comparison of injection pressure at **(a)** P=50 bars (SK1) and **(b)** P=10 bars (SK2)

From test (a), FW injection reached its plateau after 1.6 PV injected and 63.4 %OOIP recovery. From test (b), FW injection reached its plateau after 2.2 PV injected and 65.2 %OOIP recovery. So, the low pressure set up reached the plateau after 0.6 more PV injected compared to the high pressure set up. However, the recovery during low pressure FW

injection was 1.8 %OOIP more compared to the high pressure set up. The difference is not significant, and the tests should be redone and verified before any conclusions are drawn.

After switching to CFW injection we can see that the %OOIP recovery for test (a) catches up to test (b) quickly. The total CFW injection led to 8.7 %OOIP extra recovery for SK1, while it led to 10.0 %OOIP extra recovery for SK2. However, as mentioned in section 4.1.1 there were some problems during the high-pressure FI test, and the test was prematurely stopped before reaching the final plateau. The trend suggests that the recovery during CFW injection of SK1 had the potential to recover significantly more oil before the test had to be stopped, consequently it cannot be used to compare the result of total recovery from CFW injection in SK2.

In summary, the trend looks similar for both tests with the high pressure set up having a bit lower %OOIP recovery during FW injection. As test (a) switched to CFW injection the recovery rate was higher than for test (b) before the high pressure set up experienced pressure build up. The high recovery rate for CFW during high pressure injection can be linked to an increased solubility of $CO_2$ in the FW. Higher pressure leads to increased solubility and promotes better contact between CFW and the oil, causing mobilization of residual oil.

Figure 4.13 shows a clear difference between the SK1 core sample exposed to high confining pressure of 70 bars, compared to the SK2 core sample exposed to low confining pressure of 15 bars. SK1 exceeded yield pressure and led to disintegration of the core, whereas SK2 is intact.


**Figure 4.13 (a)** SK1 after high pressure FI test **(b)** SK2 after low pressure FI test

### 4.3.3 Effect of injection mode on oil recovery

CFW was injected in both secondary and tertiary mode to see the effect of injection mode. Figure 4.14 demonstrates the impact of CFW injection mode. In the case of secondary mode injection from test (a), the total recovery reached 75.7 %OOIP after injecting 2.2 PV, while in the tertiary mode from test (b), the total recovery reached 75.2 %OOIP after injecting 6.6 PV. Notably, the secondary mode CFW injection resulted in a slightly higher recovery of 0.5 %OOIP. However, it is interesting to observe that the tertiary mode CFW injection required an additional 3.6 PV of CFW to reach the plateau, which is 1.4 PV more than the secondary mode CFW injection.

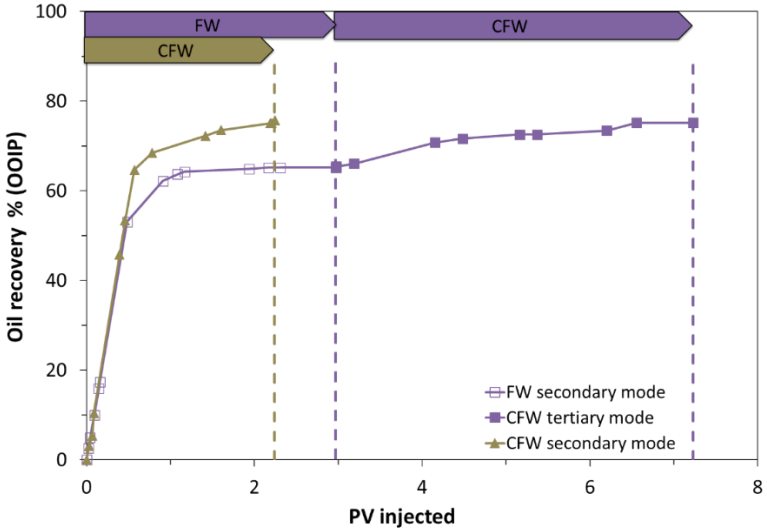


**Figure 4.14** Injection mode effect on oil recovery. Tests conducted at T=70℃ and P=10 bars. Comparison of CFW-injection in **(a)** secondary mode (SK3) **(b)** tertiary mode (SK2)

The WBT point was measured at 0.5 PV injected and a recovery of 53.1 %OOIP for secondary mode FW injection, whereas it was measured at around 0.6 PV injected and a recovery of 64.7 OOIP% for secondary mode CFW injection. The graph indicates that the trend is similar up to the WBT point, but the recovery rate is significantly higher after that point for secondary mode CFW injection compared to secondary mode FW injection. This observation is reasonable since the effect of CFW becomes more prominent when both oil and water are displaced.

In summary, the %OOIP recovery achieved with CFW injection in secondary mode is nearly identical to that of CFW injection in tertiary mode. Also, the secondary mode CFW injection reaches the final plateau much earlier, requiring less total injection volume. The tertiary mode injection, on the other hand, necessitates a longer injection duration, with 4.3 PV more injected before reaching the plateau. Additionally, the CFW injection volume alone is 1.4 PV higher for tertiary mode. Despite this, secondary mode CFW injection yields a similar OOIP% recovery compared to tertiary mode CFW injection.

This analysis suggests that in these specific experimental conditions of the study, secondary mode CFW injection shows a favorable performance in terms of reaching the plateau earlier and achieving comparable oil recovery compared to tertiary mode CFW injection. Thus, reducing the volume of water injected and produced, which in turn means less water treatment and therefore reduced $CO_2$ emissions. In addition to using some $CO_2$ in the injection water.

### 4.3.4 Spontaneous imbibition effect on total oil recovery

As mentioned, two cores were exposed to SI before the FI test. The effect of SI on total recovery will be discussed in this subchapter, both with CFW injection in secondary and tertiary mode. Figure 4.15 is a comparison of the results from FI test of CFW injection in secondary mode done on SK3 and SK4. Before the FI test started, SK4 was exposed to SI, contrary to SK3. The total recovery from SK3 reached 75.7 %OOIP after 2.2 PV injected, while the total recovery from SK4 reached 72.8 %OOIP after 2.5 PV injected. An additional 0.6 PV of CFW was injected after SK4 reached its plateau.

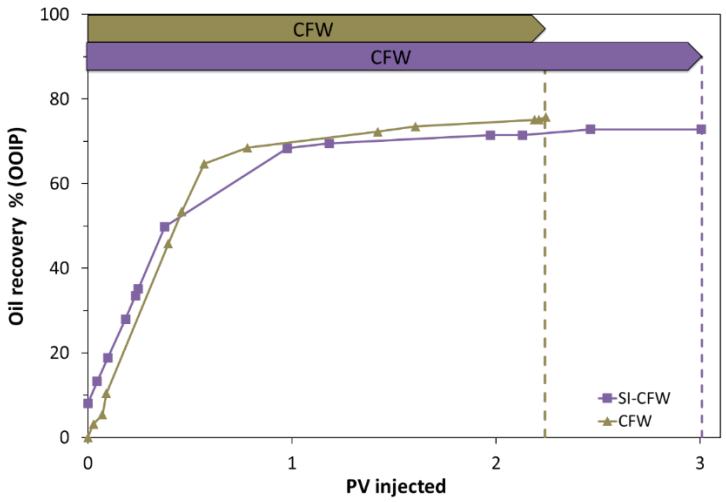


**Figure 4.15** Tests conducted at T=70℃ and P=10 bars. FI with CFW injection in secondary mode **(a)** without SI (SK3) **(b)** after SI (SK4)

As mentioned in section 4.2.4, the exact WBT point of SK4 could not be measured as it happened late in the evening, but the last point before WBT was measured at 0.4 PV of CFW injected and a recovery of 49.8 %OOIP, while SK3 reached the WBT point after 0.6 PV of CFW injected and a recovery of 64.7 %OOIP. It is clear that the WBT point happened earlier for SK4 compared to SK3, since it already recovered some of the oil during SI.

CFW injection in tertiary mode was also conducted after SI. Figure 4.16 is a comparison of the results from FI test of CFW injection in tertiary mode done on SK5 and SK2. Before the FI test started, SK5 was exposed to SI, contrary to SK2. The total recovery from SK2 reached 75.20 %OOIP after 6.6 PV injected, while the total recovery from SK5 reached 74.9 %OOIP% after 5.44 PV injected.

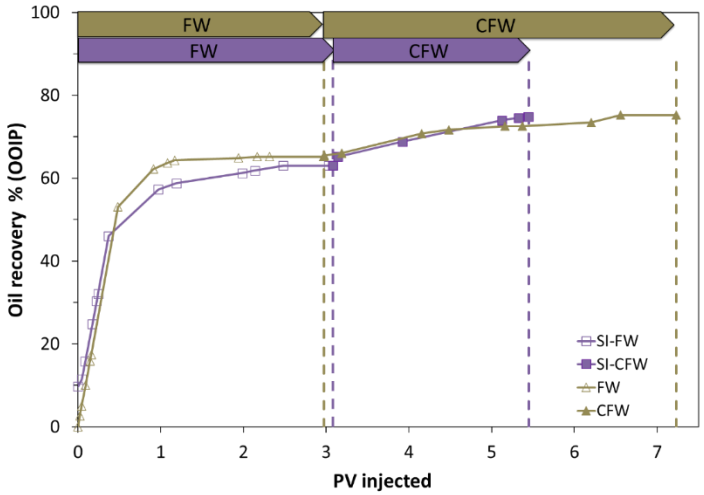


**Figure 4.16** Tests conducted at T=70℃ and P=10 bars. FI with CFW injection in tertiary mode **(a)** without SI (SK2) **(b)** after SI (SK5)

SK5 reached the WBT point after 0.4 PV of FW injected and a recovery of 46.1 %OOIP, while SK2 reached the WBT point after 0.5 PV of FW injected and a recovery of 53.1 %OOIP. The trend is the same as for CFW injection in secondary mode, where the core exposed to SI beforehand reached WBT earlier and after a lower total %OOIP recovery. This may be a consequence of the SI establishing a preferential pathway for water flow, reducing the resistance during FI. Therefore, injected water may flow easily through the core, leading to earlier breakthrough compared to the cores that were not exposed to SI beforehand.

FW injection in secondary mode reached its plateau after 2.5 PV injected and recovery of 63.0 %OOIP for SK5, while it reached its plateau after 3.0 PV injected and recovery of 65.2 %OOIP. This correlates well with the theory; SI preconditions the pores inside SK5 by partially saturating it with water.

After switching to CFW injection one can again see that the $CO_2$ mobilizes the trapped oil, and the total recovery is almost the same for SK5 and SK2, even though there were some differences after FW injection. So, a higher fraction of the recovery is caused by CFW for the cores that were exposed to SI. This is a clear indication of the effect of CFW injection. Both figures 4.15 and 4.16 demonstrate clearly that CW mobilizes the trapped oil, by $CO_2$ dissolving and swelling the oil.

### 4.3.5 Effect of injection mode after spontaneous imbibition

Figure 4.17 compares the results of the two cores that were exposed to SI before FI, SK4 and SK5. The graph represents the recovery percentage of original oil in place, %OOIP, as a function of the time (days). Both the recovery during SI and FI is compared.

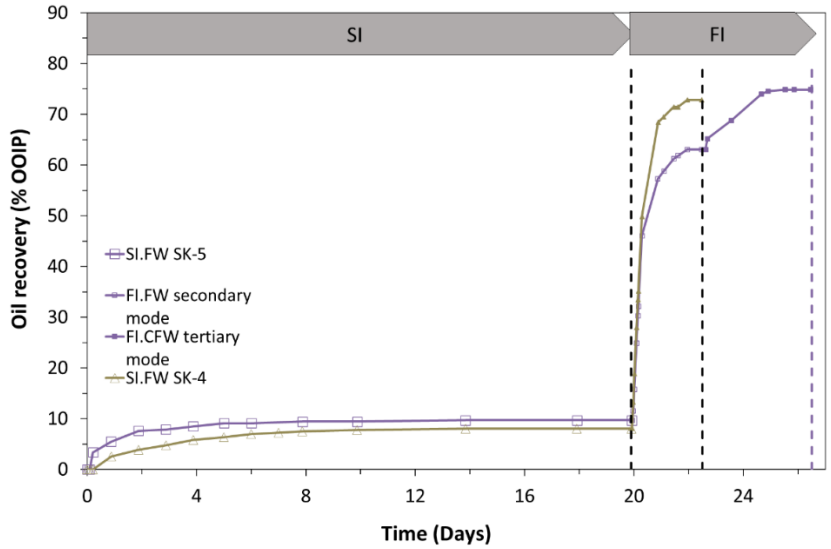


**Figure 4.17** FI injection mode effect on oil recovery after SI. Tests conducted at T=70℃ and P=10 bars. Comparison of CFW-injection in **(a)** secondary mode (SK4) **(b)** tertiary mode (SK5)

Both cores reached a plateau after 14 days of the SI test, and both tests were stopped after 20 days. Results from the SI tests were similar for SK4 and SK5, with a recovery of 8.0 %OOIP and 9.7 %OOIP, respectively.

As mentioned in section 4.2.3, this suggests that the preparation process of the cores was dependable and consistent. Different injection strategies were conducted during FI, CFW was injected into SK4 in secondary mode, while tertiary mode CFW injection was used on SK5. So, the results should be comparable to section 4.3.3.

SK4 was only exposed to CFW injection in secondary mode during the FI test. The oil recovery test for SK4 ended after 3 days of FI, and a total of 23 days including SI test. 3.0 PV of CFW was injected during this test and the recovery was 72.8 %OOIP. Plateau was reached after 2.5 PV of CFW injected.

SK5 was however exposed to FW injection beforehand in secondary mode, and CFW injection in tertiary mode during the FI test. The oil recovery test for SK5 ended after 6 days of FI, and a total of 26 days including SI test. 5.5 PV of FW and CFW was injected during this test and the recovery was 74.9 %OOIP. Plateau was reached after 2.5 PV of FW injected, the same as for CFW plateau for SK4. 2.4 PV of CFW was then injected after FW, before final plateau and recovery was reached.

The SI recovery was 1.7 %OOIP higher for SK5 than for SK4, while the total recovery of SK5 was 2.1 %OOIP higher than for SK4. So, the recovery during FI test was almost identical for

the two cores. The trend is similar to section 4.3.3, but the WBT point in this experiment seemed to come earlier and after a lower recovery %OOIP. As mentioned in section 4.3.4, this may be an effect of the SI preconditioning the pores inside SK5 and SK4 by partially saturating it with water. So, water will flow easier through the core.

To summarize, the results from this section can be used to compare with the results from section 4.3.3. From the results of both sections CFW injection in secondary mode shows favorable performance in reaching the plateau much earlier without it effecting the total %OOIP recovery. Thus, reducing water treatment and emissions.

# 5. Conclusion

Five different injection strategies using CW have been explored in this thesis. All the tests were done at 70℃. One of the tests was done on a high-pressure set up to explore the effect of pressure. Two of the cores were exposed to SI beforehand, to analyze the wettability condition and better see the effect of CFW injection. The SI tests were compared to similar studies done at higher temperature of 110℃ and using an oil with lower AN. The FI results were also compared to a similar study done at higher temperature of 130℃ and using an oil with lower AN. The CW was injected both in secondary and tertiary mode to compare the difference.

- SI on oil with a lower AN gave a much higher recovery than for oil with a higher AN. Suggesting that a lower AN gives a much stronger water-wet system. This is consistent with previously published studies.
- Wettability influenced the FW injection in secondary mode, but the CW altered the wettability in tertiary mode causing the total recovery to be similar for the weaker water-wet system compared to the stronger water-wet system. This suggests that wettability alteration was the main CWI mechanism in these studies.
- Temperature did not seem to have an impact in this study. As the results of tertiary mode CFW injection at 70℃ was compared with tertiary mode CFW injection at 130℃ conducted by Khan et al. (2023). Both the results of total oil recovery, %OOIP, and water injected were very similar for the two tests.
- Total oil recovery was similar when using CFW in secondary and tertiary mode, but secondary mode CFW required much less volume of water injected. Less water treatment suggests that secondary mode CFW injection is the most environmentally friendly and viable strategy.
- The WBT point on the high-pressure set-up was measured at highest %OOIP recovery of the strategies used. It is difficult to conclude since the test had to be prematurely stopped, but the recovery rate right after switching to CFW was very high and showed great promise. The high recovery rate might be because more $CO_2$ was dissolved in the brine.
- The WBT point was observed at the lowest %OOIP recovery for the two cores that were exposed to SI before FI test. This may be a direct consequence of the SI test preconditioning the cores by partially saturating it with FW before FI, making it easier for the water to flow through the core.

# 6. Research and development

- CFW injection at high pressure showed great promise before getting prematurely CFW injection showed great promise for the high-pressure set-up before prematurely stopping due to pressure build-up. It would be interesting to try it again with new guidelines:
    - Increasing the confining pressure stepwise to avoid the core exceeding yield stress, to avoid too high differential pressure from outside and inside the core.
    - Trying new membranes that better can withstand high pressure, so to avoid blockage of the backpressure valve.
- Repeating experiments where high pressure is compared to low pressure injection. To check if the amount of $CO_2$ in the water plays an important role.
- More studies on oils with different AN to verify the effect of wettability alteration.
- Combining smart water and CW technique to form carbonated smart water. Check the effect of $CO_2$ in different types of water, like low salinity water and SW.

# 7. References


Ahmed, T. (2019). Chapter 4 - Fundamentals of Rock Properties. In T. Ahmed (Ed.), *Reservoir Engineering Handbook (Fifth Edition)* (pp. 167-281). Gulf Professional Publishing. https://doi.org/https://doi.org/10.1016/B978-0-12-813649-2.00004-9

Ahr, W. M. (2008). Chapter 1 - Introduction. In *Geology of Carbonate Reservoirs : The Identification, Description and Characterization of Hydrocarbon Reservoirs in Carbonate Rocks* (pp. 1-12). John Wiley & Sons, Incorporated. http://ebookcentral.proquest.com/lib/uisbib/detail.action?docID=353332

Al-Shargabi, M., Davoodi, S., Wood, D. A., Rukavishnikov, V. S., & Minaev, K. M. (2022). Carbon Dioxide Applications for Enhanced Oil Recovery Assisted by Nanoparticles: Recent Developments. *ACS Omega*, *7*(12), 9984-9994. https://doi.org/10.1021/acsomega.1c07123

Alagorni, A., Yaacob, Z., & Nour, A. (2015). An Overview of Oil Production Stages: Enhanced Oil Recovery Techniques and Nitrogen Injection. *International Journal of Environmental Science and Development*, *6*, 693-701. https://doi.org/10.7763/IJESD.2015.V6.682

Amott, E. (1959). Observations relating to the wettability of porous rock. *Transactions of the AIME*, *216*(01), 156-162.

Bagrintseva, K. I. (2015). *Carbonate Reservoir Rocks*. Wiley. https://doi.org/10.1002/9781119084006

Bello, A., Ivanova, A., & Cheremisin, A. (2023). Foam EOR as an Optimization Technique for Gas EOR: A Comprehensive Review of Laboratory and Field Implementations. *Energies*, *16*, 972. https://doi.org/10.3390/en16020972

Bisweswar, G., Al-Hamairi, A., & Jin, S. (2020). Carbonated water injection: an efficient EOR approach. A review of fundamentals and prospects. *Journal of Petroleum Exploration and Production Technology*, *10*(2), 673-685. https://doi.org/10.1007/s13202-019-0738-2

Bjorlykke, K. (2010a). Chapter 1 - Introduction to petroleum geology. In *Petroleum geoscience: From sedimentary environments to rock physics* (pp. 1-31). Springer Science & Business Media.

Bjorlykke, K. (2010b). Chapter 5 - Carbonate sediments. In *Petroleum geoscience: From sedimentary environments to rock physics*. Springer Science & Business Media.

Craft, B., & Hawkins, M. (2015a). Chapter 8 - Single-phase fluid flow in reservoirs. In *Applied Petroleum Reservoir Engineering (Third edition)* (pp. 227-294).

Craft, B., & Hawkins, M. (2015b). Chapter 11 - Enhanced oil recovery. In *Applied Petroleum Reservoir Engineering (Third edition)* (pp. 405-436).

Dandekar, A. Y. (2013). Chapter 7 - Interfacial Tension and Wettability. In *Petroleum Reservoir Rock and Fluid Properties* (pp. 125-164).

Donaldson, E. C., Thomas, R. D., & Lorenz, P. B. (1969). Wettability determination and its effect on recovery efficiency. *Society of Petroleum Engineers Journal*, *9*(01), 13-20.

Drexler, S., Hoerlle, F., Godoy, W., Boyd, A., & Couto, P. (2020). Wettability Alteration by Carbonated Brine Injection and Its Impact on Pore-Scale Multiphase Flow for Carbon Capture and Storage and Enhanced Oil Recovery in a Carbonate Reservoir. *Applied Sciences*, *10*(18), 6496. https://www.mdpi.com/2076-3417/10/18/6496

Fanchi, J. (2010). Chapter 10 - Rock-fluid interactions. In *Integrated Reservoir Asset Management : Principles and Best Practices* (pp. 167-186). Elsevier Science & Technology. http://ebookcentral.proquest.com/lib/uisbib/detail.action?docID=648751

Fanchi, J. R., & Christiansen, R. L. (2016a). Introduction. In *Introduction to petroleum engineering* (pp. 1-22). John Wiley & Sons.

Fathi, S. J., Austad, T., & Strand, S. (2010). “Smart Water” as a Wettability Modifier in Chalk: The Effect of Salinity and Ionic Composition. *Energy & Fuels*, *24*(4), 2514-2519. https://doi.org/10.1021/ef901304m

Fathi, S. J., Austad, T., Strand, S., & Puntervold, T. (2010). Wettability alteration in carbonates: The effect of water-soluble carboxylic acids in crude oil. *Energy & Fuels*, *24*(5), 2974-2979.

Frykman, P. (2001). Spatial variability in petrophysical properties in Upper Maastrichtian chalk outcrops at Stevns Klint, Denmark. *Marine and Petroleum Geology - MAR PETROL GEOL*, *18*, 1041-1062. https://doi.org/10.1016/S0264-8172(01)00043-5

Gbadamosi, A. O., Junin, R., Manan, M. A., Agi, A., & Yusuff, A. S. (2019). An overview of chemical enhanced oil recovery: recent advances and prospects. *International Nano Letters*, *9*(3), 171-202. https://doi.org/10.1007/s40089-019-0272-8

Ghosh, B., Kilybay, A., Thomas, N. C., Haroun, M., Rahman, M. M., & Belhaj, H. (2022). Hybrid Carbonated Engineered Water as EOR Solution for Oil-Wet Carbonate Formation. *Energies*, *15*(21), 7889. https://www.mdpi.com/1996-1073/15/21/7889

Green, D. W., & Willhite, G. P. (2018a). Chapter 1 - Introduction to Eor Processes. In *Enhanced Oil Recovery* (pp. 1-14). Society of Petroleum Engineers. https://doi.org/10.2118/9781613994948-01

Green, D. W., & Willhite, G. P. (2018b). Chapter 2 - Microscopic Displacement of Fluids in a Reservoir. In *Enhanced Oil Recovery* (pp. 15-44). Society of Petroleum Engineers. https://doi.org/10.2118/9781613994948-02

Green, D. W., & Willhite, G. P. (2018c). Chapter 4 - Macroscopic Displacement of Fluids in a Reservoir. In *Enhanced Oil Recovery* (pp. 101-138). Society of Petroleum Engineers. https://doi.org/10.2118/9781613994948-04

Hamouda, A. A., & Bagalkot, N. (2019). Effect of Salts on Interfacial Tension and CO2 Mass Transfer in Carbonated Water Injection. *Energies*, *12*(4), 748. https://www.mdpi.com/1996-1073/12/4/748

Khan, M. A. I., Sander Haaland, K., Ivan Dario Pinerez, T., Puntervold, T., & Strand, S. (2023, 2023). Carbonated Smart Water Injection for Optimized Oil Recovery in Chalk at High Temperature. Les Ulis.

Kokal, S., & Al-Kaabi, A. (2010). Enhanced oil recovery: challenges & opportunities. *World Petroleum Council: Official Publication*, *64*, 64-69.

Lake, L. W. (2010). Chapter 3 - Petrophysics and petrochemistry. In *Enhanced oil recovery* (pp. 43-88). Society of Petroleum Engineers.

Lucia, F. J. (2007). Chapter 4 - Depositional textures & petrophysics. In *Carbonate reservoir characterization : an integrated approach* (2nd ed., pp. 111-142). Springer.

Manrique, E., Thomas, C., Ravikiran, R., Izadi, M., Lantz, M., Romero, J., & Alvarado, V. (2010). EOR: Current Status and Opportunities. SPE Improved Oil Recovery Symposium,

Mazzullo, S. J., Chilingarian, G. V., & Bissell, H. J. (1992). Chapter 2 Carbonate Rock Classifications. In G. V. Chilingarian, S. J. Mazzullo, & H. H. Rieke (Eds.), *Developments in Petroleum Science* (Vol. 30, pp. 59-108). Elsevier. https://doi.org/https://doi.org/10.1016/S0376-7361(09)70125-6

Morrow, N. R., & Mason, G. (2001). Recovery of oil by spontaneous imbibition. *Current Opinion in Colloid & Interface Science*, *6*(4), 321-337. https://doi.org/https://doi.org/10.1016/S1359-0294(01)00100-5

Mousavi Moghadam, A., & Salehi, M. (2019). Enhancing hydrocarbon productivity via wettability alteration: A review on the application of nanoparticles. *Reviews in Chemical Engineering*, *35*. https://doi.org/10.1515/revce-2017-0105

Perkins, E., & Innovates, A. (2003). Fundamental geochemical processes between CO2, water and minerals. *Alberta Innovates–Technology Futures*.

Piñerez Torrijos, I. D. (2017). *Enhanced oil recovery from sandstones and carbonates with "Smart Water"* University of Stavanger, Faculty of Science and Technology, Department of Petroleum Engineering]. Stavanger.

Puntervold, T., Strand, S., & Austad, T. (2007). New Method To Prepare Outcrop Chalk Cores for Wettability and Oil Recovery Studies at Low Initial Water Saturation. *Energy & Fuels - ENERG FUEL*, *21*. https://doi.org/10.1021/ef700323c

Reed, J., Birkeland, K., Bratteli, F., Howard, J., Maas, J., & Springer, N. (2014). *Advanced Core Measurements "Best Practices" for Low Reservoir Quality Chalk*.

Rezaei Doust, A., Puntervold, T., Strand, S., & Austad, T. (2009). Smart Water as Wettability Modifier in Carbonate and Sandstone: A Discussion of Similarities/Differences in the Chemical Mechanisms. *Energy & Fuels*, *23*(9), 4479-4485. https://doi.org/10.1021/ef900185q

Riazi, M., Sohrabi, M., Jamiolahmady, M., Ireland, S., & Brown, C. (2009). *Oil Recovery Improvement Using CO2-Enriched Water Injection*.

Ruidiaz, E. M., Winter, A., & Trevisan, O. V. (2018). Oil recovery and wettability alteration in carbonates due to carbonate water injection. *Journal of Petroleum Exploration and Production Technology*, *8*(1), 249-258. https://doi.org/10.1007/s13202-017-0345-z

Sagbana, P. I., Sarkodie, K., & Nkrumah, W. A. (2022). A critical review of carbonate reservoir wettability modification during low salinity waterflooding. *Petroleum*. https://doi.org/https://doi.org/10.1016/j.petlm.2022.01.006

Sanni, M. (2018). Petroleum Reservoir Rock Properties. In (Vol. 237, pp. 17-64). United States: American Geophysical Union. https://doi.org/10.1002/9781119387985.ch2

Satter, A., Iqbal, G. M., & Buchwalter, J. L. (2008a). Chapter 2 - Rock charactertiscs, significance in petroleum reservoir, and applications. In *Practical enhanced reservoir engineering : assisted with simulation software* (pp. 17-99). PennWell Corp.

Satter, A., Iqbal, G. M., & Buchwalter, J. L. (2008c). Chapter 16 - Improved oil recovery processes: Fundamentals of waterflooding and applications. In *Practical enhanced reservoir engineering : assisted with simulation software* (pp. 491-548). PennWell Corp.

Seyyedi, M., Sohrabi, M., & Farzaneh, A. (2015). Investigation of Rock Wettability Alteration by Carbonated Water through Contact Angle Measurements. *Energy & Fuels*, *29*(9), 5544-5553. https://doi.org/10.1021/acs.energyfuels.5b01069

Sheng, J. J. (2013). Chapter 12 - Surfactant Enhanced Oil Recovery in Carbonate Reservoirs. In J. J. Sheng (Ed.), *Enhanced Oil Recovery Field Case Studies* (pp. 281-299). Gulf Professional Publishing. https://doi.org/https://doi.org/10.1016/B978-0-12-386545-8.00012-9

Sohrabi, M., Riazi, M., Jamiolahmady, M., Ireland, S., & Brown, C. (2009). *Mechanisms of Oil Recovery by Carbonated Water Injection*.

Soleimani, P., Shadizadeh, S. R., & Kharrat, R. (2021). Experimental assessment of hybrid smart carbonated water flooding for carbonate reservoirs. *Petroleum*, *7*(1), 80-90. https://doi.org/https://doi.org/10.1016/j.petlm.2020.03.006

Standnes, D. C., & Austad, T. (2000). Wettability alteration in chalk: 1. Preparation of core material and oil properties. *Journal of Petroleum Science and Engineering*, *28*(3), 111-121. https://doi.org/https://doi.org/10.1016/S0920-4105(00)00083-8

Tarek, A., & Meehan, D. N. (2012). Chapter 4 - Performance of Oil Reservoirs. In *Advanced Reservoir Management and Engineering* (Second Edition ed., pp. 433-483). Elsevier Inc. https://doi.org/10.1016/B978-0-12-385548-0.00004-X

Teklu, T. W., Alameri, W., Kazemi, H., & Graves, R. (2015). *Contact Angle Measurements on Conventional and Unconventional Reservoir Cores*. https://doi.org/10.2118/178568-MS

Yao, Y., Wei, M., & Kang, W. (2021). A review of wettability alteration using surfactants in carbonate reservoirs. *Advances in Colloid and Interface Science*, *294*, 102477. https://doi.org/https://doi.org/10.1016/j.cis.2021.102477

Zhang, P., Tweheyo, M. T., & Austad, T. (2007). Wettability alteration and improved oil recovery by spontaneous imbibition of seawater into chalk: Impact of the potential determining ions Ca2+, Mg2+, and SO42−. *Colloids and Surfaces A: Physicochemical and Engineering Aspects*, *301*(1), 199-208. https://doi.org/https://doi.org/10.1016/j.colsurfa.2006.12.058

# A. Appendix

## A.1 Calculations

Examples of calculations made will be presented in this section. All done on SK1.

### A.1.1 Porosity

An example of porosity calculation is presented. Porosity was calculated using equations 2.1 and 3.2.

The total volume of the core:

$$V_T = L * \pi * \left(\frac{D}{2}\right)^2 = 6.89\ cm * \pi * \left(\frac{3.8\ cm}{2}\right)^2 = 78.14\ ml$$

Pore volume of the core:

$$V_P = \frac{m_s - m_{dry}}{\rho_{10*diluted\ FW}} = \frac{144.55\ g - 106.03\ g}{1.0026\ g/ml} = 38.42\ ml$$

Porosity of the core:

$$\phi = \frac{V_P}{V_T} * 100\% = \frac{38.42\ ml}{78.14\ ml} * 100\% = \mathbf{49.17\%}$$

### A.1.2 Permeability

Permeability was calculated using equation 2.2.

Cross-sectional area:

$$A = \pi * \left(\frac{D}{2}\right)^2 = \pi * \left(\frac{3.8}{2}\right)^2 = 11.34\ cm$$

For injection rate, q=0.1 ml/min, converted to $m^3$/sec:

$$k = \frac{q*\mu*L}{A*\Delta p} = \frac{(1.7*10^{-9})*0.0009*0.0689}{0.0011341*29700} = \mathbf{3.13 * 10^{-15}\ m^2}$$

Repeat the process for injection rate, q=0.15 ml/min, take the average, and convert to mD.

## A.2 Oil recovery data

Results from the oil recovery tests will be presented in this section. Yellow shading indicates a change in injection fluid.

### A.2.1 High injection pressure

Data from the high-pressure FI test is presented in table A.1.

**Table A.1** 1st test. High pressure FI by FW → CFW (SK1)

| Pore volume injected | Oil produced [ml] | | Recovery [%OOIP] |
|---|---|---|---|
| | FW in secondary mode | CFW in tertiary mode | |
| 0.00 | 0.0 | | 0.0 |
| 0.03 | 1.0 | | 2.9 |
| 0.06 | 2.0 | | 4.9 |
| 0.15 | 4.9 | | 14.2 |
| 0.23 | 7.5 | | 21.7 |
| 0.69 | 21.3 | | 61.6 |
| 1.31 | 21.8 | | 63.1 |
| 1.62 | 21.9 | | 63.4 |
| 1.68 | 21.9 | | 63.4 |
| 2.18 | 21.9 | | 63.4 |
| 2.31 | 21.9 | | 63.4 |
| 2.63 | 21.9 | | 63.4 |
| 3.32 | 21.9 | | 63.4 |
| 3.32 | 21.9 | 0.0 | 63.4 |
| 3.39 | 21.9 | 0.1 | 63.7 |
| 4.04 | 21.9 | 2.2 | 69.7 |
| 4.13 | 21.9 | 2.3 | 70.0 |
| 4.30 | 21.9 | 2.4 | 70.3 |
| 4.44 | 21.9 | 2.7 | 71.2 |
| 5.01 | 21.9 | 3.0 | 72.1 |

### A.2.2 Low injection pressure

The data from the low-pressure FI and SI tests are presented in this section.

**Table A.2** 2nd test. Low pressure FI by FW → CFW (SK2)

| Pore volume injected | Oil produced [ml] | | Recovery [%OOIP] | ΔP [mbar] |
|---|---|---|---|---|
| | FW in secondary mode | CFW in tertiary mode | | |
| 0.00 | 0.0 | | 0.0 | 580 |
| 0.02 | 0.9 | | 2.7 | 565 |
| 0.04 | 1.6 | | 5.0 | 555 |
| 0.09 | 3.4 | | 10.0 | 539 |
| 0.15 | 5.4 | | 15.9 | 533 |
| 0.16 | 5.9 | | 17.4 | 533 |
| 0.48 | 18.0 | | 53.1 | 600 |
| 0.91 | 21.1 | | 62.2 | 525 |
| 1.08 | 21.6 | | 63.7 | 512 |
| 1.17 | 21.8 | | 64.3 | 510 |
| 1.94 | 22.0 | | 64.9 | 486 |
| 2.17 | 22.1 | | 65.2 | 482 |
| 2.31 | 22.1 | | 65.2 | 481 |
| 2.97 | 22.1 | | 65.2 | 470 |
| 2.97 | 22.1 | 0.0 | 65.2 | 80 |
| 2.98 | 22.1 | 0.1 | 65.5 | 79 |
| 3.19 | 22.1 | 0.3 | 66.1 | 1048 |
| 4.15 | 22.1 | 1.9 | 70.8 | 1002 |
| 4.48 | 22.1 | 2.2 | 71.7 | 853 |
| 5.16 | 22.1 | 2.5 | 72.5 | 961 |
| 5.37 | 22.1 | 2.5 | 72.5 | 1004 |
| 6.20 | 22.1 | 2.8 | 73.4 | 1270 |
| 6.56 | 22.1 | 3.4 | 75.2 | - |
| 7.23 | 22.1 | 3.4 | 75.2 | - |

**Table A.3** 3rd test. Low pressure FI by CFW → SW (SK3)

| Pore volume injected | Oil produced [ml] | | Recovery [%OOIP] | ΔP [mbar] |
|---|---|---|---|---|
| | CFW in secondary mode | SW in tertiary mode | | |
| 0.00 | 0.0 | | 0.0 | 382 |
| 0.03 | 1.0 | | 3.2 | 357 |
| 0.07 | 2.6 | | 5.4 | 350 |
| 0.09 | 3.3 | | 10.4 | 335 |
| 0.39 | 14.5 | | 45.8 | 826 |
| 0.46 | 16.9 | | 53.3 | 726 |
| 0.57 | 20.5 | | 64.7 | 110 |
| 0.78 | 21.7 | | 68.5 | 1145 |
| 1.42 | 22.9 | | 72.3 | 910 |
| 1.60 | 23.3 | | 73.5 | 947 |
| 2.19 | 23.8 | | 75.1 | 350 |
| 2.21 | 23.8 | | 75.1 | 310 |
| 2.24 | 24.0 | | 75.7 | 109 |
| 2.24 | 24.0 | 0.0 | 75.7 | 730 |
| 2.24 | 24.0 | 0.0 | 75.7 | 730 |
| 2.96 | 24.0 | 0.0 | 75.7 | 93 |
| 3.77 | 24.0 | 0.0 | 75.7 | 90 |

**Table A.4** 4th test. Spontaneous imbibition by FW (SK4)

| Time [days] | Oil produced [ml] | Recovery [%OOIP] |
|---|---|---|
| 0.0 | 0.0 | 0.0 |
| 0.1 | 0.0 | 0.0 |
| 0.2 | 0.0 | 0.0 |
| 0.9 | 0.9 | 2.5 |
| 1.9 | 1.4 | 3.9 |
| 2.9 | 1.7 | 4.7 |
| 3.9 | 2.1 | 5.8 |
| 5.0 | 2.3 | 6.4 |
| 6.0 | 2.5 | 6.9 |
| 7.0 | 2.6 | 7.2 |
| 7.9 | 2.7 | 7.5 |
| 9.9 | 2.8 | 7.8 |
| 13.8 | 2.9 | 8.0 |
| 17.9 | 2.9 | 8.0 |
| 19.9 | 2.9 | 8.0 |

**Table A.5** 5th test. Spontaneous imbibition by FW (SK5)

| Time [days] | Oil produced [ml] | Recovery [%OOIP] |
|---|---|---|
| 0.0 | 0.0 | 0.0 |
| 0.1 | 0.0 | 0.0 |
| 0.2 | 1.1 | 3.3 |
| 0.9 | 1.8 | 5.5 |
| 1.9 | 2.5 | 7.6 |
| 2.9 | 2.6 | 7.9 |
| 3.9 | 2.8 | 8.5 |
| 5.0 | 3.0 | 9.1 |
| 6.0 | 3.0 | 9.1 |
| 7.9 | 3.1 | 9.4 |
| 9.9 | 3.1 | 9.4 |
| 13.8 | 3.2 | 9.7 |
| 17.9 | 3.2 | 9.7 |
| 19.9 | 3.2 | 9.7 |

**Table A.6** 6th test. Low pressure FI by CFW after SI (SK4)

| Pore volume injected | Oil produced [ml] | | Recovery [%OOIP] | ΔP [mbar] |
|---|---|---|---|---|
| | SI by FW | CFW in secondary mode | | |
| 0.00 | 2.9 | 0.0 | 8.0 | 740 |
| 0.05 | 2.9 | 1.9 | 13.3 | 740 |
| 0.10 | 2.9 | 3.9 | 18.8 | 680 |
| 0.18 | 2.9 | 7.2 | 28.0 | 684 |
| 0.23 | 2.9 | 9.2 | 33.5 | 950 |
| 0.25 | 2.9 | 9.8 | 35.2 | 816 |
| 0.38 | 2.9 | 15.1 | 49.8 | 1140 |
| 0.98 | 2.9 | 21.8 | 68.4 | 605 |
| 1.18 | 2.9 | 22.2 | 69.5 | 784 |
| 1.97 | 2.9 | 22.9 | 71.4 | 880 |
| 2.13 | 2.9 | 22.9 | 71.4 | 733 |
| 2.46 | 2.9 | 23.4 | 72.8 | 908 |
| 3.01 | 2.9 | 23.4 | 72.8 | 726 |

**Table A.7** 7th test. Low pressure FI by FW→CFW after SI (SK5)

| Pore volume injected | Oil produced [ml] | | | Recovery [%OOIP] | ΔP [mbar] |
|---|---|---|---|---|---|
| | SI by FW | FW in secondary mode | CFW in secondary mode | | |
| 0.00 | 3.2 | 0.0 | | 9.7 | 611 |
| 0.04 | 3.2 | 0.6 | | 11.5 | 644 |
| 0.09 | 3.2 | 2.0 | | 15.8 | 652 |
| 0.18 | 3.2 | 5.0 | | 24.9 | 636 |
| 0.22 | 3.2 | 6.8 | | 30.3 | 632 |
| 0.24 | 3.2 | 7.4 | | 32.1 | 635 |
| 0.37 | 3.2 | 12.0 | | 46.1 | 660 |
| 0.97 | 3.2 | 15.7 | | 57.3 | 535 |
| 1.19 | 3.2 | 16.2 | | 58.8 | 529 |
| 1.98 | 3.2 | 17.0 | | 61.2 | 502 |
| 2.14 | 3.2 | 17.2 | | 61.8 | 499 |
| 2.48 | 3.2 | 17.6 | | 63.0 | 493 |
| 3.03 | 3.2 | 17.6 | | 63.0 | 466 |
| 3.08 | 3.2 | 17.6 | | 63.0 | 104 |
| 3.08 | 3.2 | 17.6 | 0.0 | 63.0 | 784 |
| 3.14 | 3.2 | 17.6 | 0.7 | 65.2 | 784 |
| 3.92 | 3.2 | 17.6 | 1.9 | 68.8 | 1028 |
| 5.12 | 3.2 | 17.6 | 3.6 | 73.9 | 1123 |
| 5.32 | 3.2 | 17.6 | 3.8 | 74.6 | 1274 |
| 5.44 | 3.2 | 17.6 | 3.9 | 74.9 | 1415 |
| 5.44 | 3.2 | 17.6 | 3.9 | 74.9 | 679 |
| 5.45 | 3.2 | 17.6 | 3.9 | 74.9 | 646 |